INVESTIGATING TRANSIENT SOLUTION PHASE ORGANIZATION USING FLUORESCENT PROBE MOLECULES

By

Joseph Jerome Tulock

A DISSERTATION

Submitted to
Michigan State University
in partial fulfillment of the requirements
for the degree of

DOCTOR OF PHILOSOPHY

Department of Chemistry

2001

ABSTRACT

INVESTIGATING TRANSIENT SOLUTION PHASE ORGANIZATION USING FLUORESCENT PROBE MOLECULES

By

Joseph Jerome Tulock

Fluorescent probes have advanced our understanding of molecular scale chemical and physical processes important in areas of research ranging from the study of transport phenomena in biological membranes and, the morphology of molecular multilayer assemblies to transient organization in the liquid phase. Molecular probes are well suited for these investigations because their emission responses are often affected by changes in their local environments such as, but not limited to, pH, polarity, dielectric response, and viscosity. As such, molecular probes report the state of their surroundings and this information can be used to understand the relationship between molecular scale interactions and the macroscopic world. Apart from their spectroscopic behavior, when present in restricted environments or a strong interaction with their environment exists, the motional dynamics of probes can also give clues to reveal the important molecular interactions driving chemical and physical processes.

The focus of this thesis is on the use of fluorescent probe molecules to investigate the spontaneous self-assembly of solutes in solution preceding crystallization. Two chemical systems are investigated. First, aqueous solutions of adipic acid are studied using the fluorescent probes 1-pyrenecarboxylic acid (PCA) and 1-pyrenebutryic acid (PBA). These probe molecules posses a carboxylic acid functionality that enables them

to act as sites for solute aggregation, enabling them to report on solute organization preceding crystallization. The steady-state and time resolved emission responses of each probe are recorded as a function of adipic acid concentration to understand their ability to report crystallization phenomena. The concentration-dependent emission responses and reorientation dynamics of these probes are compared to establish the spectroscopic and structural criteria important for fluorescent probes to sense organization in crystallizing systems.

The knowledge gained from these studies of the adipic acid systems is applied to study the hydrolytic polymerization of tetravalent zirconium (Zr^{4+}). The rotational diffusion dynamics of PCA are studied as a function of the degree of polymerization to characterize the structure of zirconium hydrous polymers forming in aqueous solutions. This study establishes the ability of fluorescent probes to report detailed structural information on the structure of solute aggregates. The work in this thesis provides the knowledge required for successful application of fluorescent probes to study solute self-assembly in a broad range of chemical systems.

To my family and friends for their love and support

ACKNOWLEDGMENTS

Foremost I would like to thank my advisor Gary Blanchard for his guidance and support during the course of my studies in graduate school. I have appreciated the genuine interest Gary has always taken in the professional development and personal success of each individual working under his direction. While working in the Blanchard group I have enjoyed the freedom to direct my own research, which has provided me with equally opportunity to learn from my successes and failures. I know that I have been extremely fortunate to have Gary as my thesis advisor. Not only has he been a tremendous resource scientifically, but his personal and down to earth way of interacting with graduate students has been a great support for me during graduate school (thanks for the fuse).

I would like to thank all of the past and current Blanchard group members that I have had the privilege of working with. These have been the people that have been kind enough to listen to hallucinations about what I thought might be happening with my data and have offered helpful suggestions and insights along the way. Having been a part of this "kinder/gentler" group has made the stress and strain of graduate school much easier to bear. Steve, Punit, and Lee deserve special recognition. They have served as my "partners in crime" during the past number of years and are responsible for the most memorable moments I have had during graduate school (Vegas, Ann Arbor, TJ, poster sessions, Canoe Bash etc.). I'm sure there will be many more in the future at various spots on the globe. I would also like to thank Carl Iverson who, through no small favor, helped lighten the load through my most difficult time during graduate school. Carl and I also

had a number of adventures together. I would also like to thank Marybeth Congdon for her love and support.

Finally, I would like to thank Nancy Stouder who instilled in me the most basic principles of dedication, perseverance, and self-reliance, which have always been the basis for my successes in life. Her sacrifices and visible demonstration of these principles have ensured my opportunities.

TABLE OF CONTENTS

List of Tables

List of Figures

Chapter 1

Introduction

Crystallization represents one of the most widely used methods for separating and purifying chemical compounds. The proliferation of this method as a means for resolving chemical components from solution is due to the relative ease with which bulk solution parameters can be varied to effect a phase change. In addition, crystallization processes are easily scalable to accommodate the production of industrially significant compounds. Typical solution parameters available for control may include temperature, solute concentration, solvent composition and pH, where appropriate[1]. Most control schemes involving these parameters have been largely based upon empiricism and the connection between molecular scale interactions responsible for solute self-assembly, crystal nucleation, and macroscopic crystal properties has not been well established. Establishing this connection is vital for controlling crystallization because crystalline products isolated under different conditions can often exhibit unique physical properties that may be crucial for a particular application. Because of the need to exert greater control over crystallization, researchers have sought to detect the onset of solute organization from solution and characterize important solvent and solute interactions that define organized solute species.

Initially, attempts to detect the onset of solute organization in solution focused on identifying changes in bulk solution properties near or above the saturation limit. Attempts to correlate changes in the viscosity, refractive index, and conductivity of saturated solutions failed to provide evidence of solute organization[2]. Mullin and Leci

obtained evidence for solute cluster formation in solutions of citric acid[3]. They found that, when allowed to stand for extended periods, isothermal columns of supersaturated citric acid solutions formed concentration gradients with the bottom portion of the column having the greatest concentration. Similar gradients were not observed for saturated or undersaturated solutions of citric acid. Larson and Garside later studied concentration gradients in supersaturated solutions (citric acid, urea, sodium nitrate, potassium sulphate, potassium nitrate) to estimate the size of solute aggregates[4,5]. Myerson examined diffusion coefficients in concentrated solutions of electrolyte and non-electrolyte solutes and found that for supersaturated solutions, diffusion coefficients decreased rapidly with increasing solute concentration[6-10]. This situation was thought to result from formation of solute aggregates. Although these experiments provided evidence of solute self-assembly preceding crystallization, they were not able to elucidate the structure of aggregates. The sensitivity of these techniques also precluded the existence of structure in undersaturated solutions to be determined.

Recently fluorescent probe molecules have been used to study crystallization phenomena[11-13]. Molecular probes are suited for the study of solution phase phenomena because the emission response of probes depends sensitively on the molecular interactions they experience while in the excited state. By nature, these interactions are transient and persist over very short time scales on the order of the fluorescence lifetime and rotational diffusion dynamics of many fluorophores. This dependence enables changes in the emission response of probe molecules to be related to the onset of molecular aggregation. The use of fluorescent probes to study solvation phenomena in simple systems, neat solvents containing probe molecules at low concentrations (~ 10^{-6}

M), has established the utility of probes to sense changes in their immediate environments and local molecular scale heterogeneity associated with solvent ordering[14]. The use of fluorescent probes to study more complex systems has also been well established. Molecular scale self-assembly has also been studied via introduction of fluorescent probes into micellar solutions[15]. Studies of the differences in emission response of probe molecules in neat solvents and in the presence of micelles have revealed important structural information regarding organization occurring in these systems.

A requirement for correlating the steady-state and transient emission responses of probes with aggregation phenomena is that the location of probes in solution be well defined. This can be accomplished by choosing probe molecules that incorporate into the crystallizing matrix selectively, with the potential to act as sites for solute aggregation. In this way the probe molecule environment is defined largely by interactions with the solute enabling the probe to sense solute assembly. Typically probes consist of highly fluorescent molecules having well characterized spectroscopic responses, which possess pendant moieties that are structurally similar to the crystallizing solute. In principle , the identity of this moiety need not resemble the solute but, only promote selective interaction of the probe molecule with the solute. It has been shown that, at sufficiently low concentrations, occlusion of such impurities within crystals can occur without significantly altering their formation[16].

This method for studying crystallization, referred to as the "lock and key" approach, has been applied previously to study crystallization phenomena in aqueous sugar solutions. Rasimas has investigated aqueous solutions of glucose using the

fluorescent probes resorufin and glycosly resorufin, the latter containing the pendant functionality enabling incorporation of the probe into glucose crystals[17]. Rotational diffusion studies performed in aqueous glucose solutions revealed the reorientation of glycosly resorufin to be anomalously slow near saturation while the native resorufin chromophore exhibited the expected behavior consistent with model predictions. The unique rotational behavior of each of these probe demonstrated the ability of "lock and key" probes to selectively incorporate into pre-crystalline aggregates. Evidence for the incorporation of the native resorufin chromophore was not observed. These results pointed to the ability of functionalized probes to detect solute assembly and act as sites for solute aggregation. In addition, significant solute ordering was detected preceding the saturation limit.

The work presented in this thesis represents an extension of the "lock and key" approach to study two different chemical systems, aqueous solutions of adipic acid and tetravalent zirconium (Zr^{4+}). The probe molecules used for this work are 1-pyrenecaryboxylic acid (PCA, Figure 1) and 1-pyrenebutyric acid (PBA, Figure 1). Both probes were used for study of the adipic acid system and PCA has been used to investigate zirconium solutions. Organization in the adipic acid system is the result of intermolecular interactions, which are dynamical in nature, as a result, aggregates that form are short lived. The zirconium ion undergoes hydrolytic polymerization producing hydrous zirconia polymers. These structures are formed through chemical bonds and persist over long times. One issue concerning the "lock and key" approach is the feasibility of its application to a variety of chemical systems. In light of this it is important to understand what affect the identity of the probe molecule or the solute will

have on the efficacy of this approach to report on pre-crystalline phenomena. Because of their unique properties, solutions of adipic acid and zirconium have been chosen for this work to explore these issues. The specific questions addressed in each chapter are discussed below.

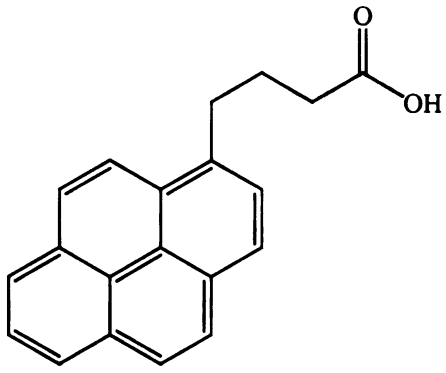

1-pyrenebutyric acid (PBA)

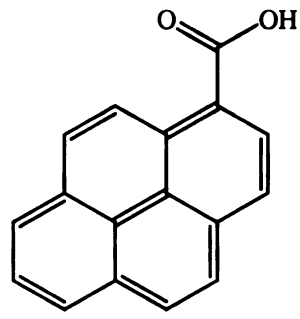

1-pyrenecarboxylic acid (PCA)

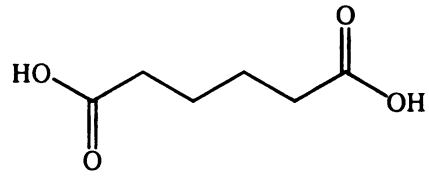

adipic acid

Figure 1.1 Structures of 1-pyrenecarboxylic acid (HPCA), 1-pyrenebutyric acid (HPBA), and adipic acid.

Chapter 2 is a study of the steady-state spectroscopy and rotational diffusion dynamics of PCA in solutions of adipic acid to characterize pre-crystalline aggregates in carboxylic acid systems. The probe is found to undergo complexation with the solute and

the steady-state emission response of PCA is used to characterize this interaction. Fluorescence lifetimes were found to be sensitive to solute concentration and an indicator of proximity to saturation. The discontinuous behavior of this response in the region of saturation indicates the ability of PCA to sense local organization associated with solute assembly. Rotational diffusion measurements detected the onset of organization at concentrations preceding saturation and indicate the "average" size of aggregates. The persistence time of aggregates was established as being at least 100 ps but less that 5 ns.

Chapter 3 details the use of PBA to study the adipic acid system discussed in chapter 2. The focus of chapter 3 is a comparative analysis of the role of probe identity in investigating spontaneous solute self-assembly. The main points addressed in this chapter are (1) What is the consequence of spectroscopically isolating the pendant functionality from the probe chromophore? (2) What effect does placing the chromophore from the site of solute aggregation have on the probe's ability to sense aggregation? (see Figure 1). In order to resolve these issues, similar experiments to those discussed in chapter 2 are performed, substituting PBA as the probe molecule, and compared to those using PCA as the probe molecule. From the emission spectra and fluorescence lifetimes of PBA in adipic acid solutions it was found that absence of conjugation between the pyrene chromophore and carboxylic acid moiety limits the ability of this probe to sense solution composition and aggregation phenomena. The rotational diffusion data acquired with PBA indicate the formation of solute aggregates but were less detailed than those data obtained with PCA. This was determined to be the result of PBA possessing greater conformational freedom between the chromopore and aggregation site.

Chapter 4 is a study of the use of PCA to investigate structure in aqueous solutions of the tetravalent metal ion Zr^{4+}. The focus of this chapter is on understanding the limit of structural information that fluorescent probes can report on solute self-assembly. A number of aspects concerning the aqueous chemistry of zirconium have been established and serve as a reference point for evaluating the "lock and key" strategy. Zr^{4+} undergoes hydrolysis to form hydrous oxide polymers. While the extent of this polymerization is expected to increase upon heating solutions of zirconium[18-23], the structure of these polymeric species has not been characterized fully. Whatever their structure, polymers persist longer that the dynamical behavior of probes enabling greater correlation between the probes emission response and aggregate structure to be made. The lifetime and rotational diffusion dynamics of PCA are recorded at various stages of polymer growth. The lifetime data are found to be sensitive to changes in pH caused by the hydrolytic polymerization of Zr^{4+} thereby sensing the completion of the polymerization process. The rotational data demonstrate that polymers achieve a constant size in solution, the upper bound of which lies in the range of 2,900$Å^3$-24,000 $Å^3$ and likely are of cylindrical symmetry. The findings reported in chapter 4 demonstrate the ability of fluorescent probes to report on the dimensions of structure associated with spontaneous solute self-assembly.

Chapter 5 summarizes the findings of chapters 2-4 and describes the potential use of chemically modified surfaces for templating crystal growth. These surfaces may play a significant role in the construction of zirconium phosphonate multilayer assemblies.

Literature Cited

1. Mersmann, A., ed. *Crystallization Technology Handbook.* 1995, Marcel Dekker, Inc.: New York.

2. Narayan, H.; Youngquist, G. R. *AIChE Symposium Series* **1987**. *253*(1).

3. Mullin, J. W.; Jeci, C. *Philos. Mag.* **1969**. *19*(1075).

4. Larson, M. A.; Garside, J. *Chemical Engineering Science* **1986**. *41*(5): p. 1285-1289.

5. Larson, M. A.; Garside, J. *J. Crystal Growth* **1986**. *76*: p. 88.

6. Chang, Y. C.; Myerson, A. S. *AIChE Journal* **1986**. *32*(9).

7. Myerson, A. S.; Chang, Y. C. *AIChE Journal* **1986**. *32*(10): p. 1747.

8. Myerson, A. S.; LO, Y. P. *J. Crystal Growth* **1990**. *99*: p. 1048-1052.

9. Myerson, A. S.; Ginde, R. M. *J. Crystal Growth* **1992**. *116*: p. 41-47.

10. Sorell, L. S.; Myerson, A. S. *AIChE Journal* **1982**. *28*(5): p. 772-778.

11. Pan, B.; Chakraborty, R.; Berglund, K. A. *J. Crystal Growth* **1993**. *130*: p. 587-599.

12. Chakraborty, R.; Berglund, K. A. *AIChE Symposium Series* **1991**. *284*: p. 113.

13. Chakraborty, R.; Berglund, K. A. *J. Crystal Growth* **1992**. *125*: p. 81-96.

14. Blanchard, G. J. *Journal of Chemical Physics* **1987**. *87*(12): p. 6802-6808.

15. Kalyanasundaram, K., *Photchemistry in Microheterogeneous Systems.* 1987, New York: Harcourt Brace Jovanovich, Publishers.

16. Weissbuch, I.; Addadi, L.; Leiserowitz, L.; Lahav, M. *J. Am. Chem. Soc.* **1988**. *110*: p. 561-567.

17. Rasimas, J. P.; Berglund, K. A.; Blanchard, G. J. *Journal of Physical Chemistry* **1996**. *100*(42): p. 17034-17040.

18. Clearfield, A. *Inorganic Chemistry* **1964**. *3*(1): p. 146-148.

19. Clearfield, A. *Rev.Pure and Appl. Chem.* **1964**. *14*(91): p. 91-108.

20. Clearfield, A. *J.Mater.Res* **1990**. *5*(1): p. 161-162.

21. Bilinsnki, H.; Durfor, C.; Tyree, S. Y. J. *J. Inorg. Nucl. Chem.* **1977**. *39*: p. 1637-1640.

22. Mukherji, A. K., *Analytical Chemistry of Zirconium and Hafnium*. 1970, New York: Pergamon Press.

23. Singhal, A.; Toth, L. M.; Beaucage, J.-s. L.; Peterson, J. *Journal of Colloid and Interface Science* **1997**. *194*: p. 470-481.

Chapter 2

Measuring Aggregation in Aqueous Adipic Acid Solutions Using a Lock-and-Key Probe Molecule

SUMMARY

In this chapter we report on the measurement of molecular scale self-organization of aqueous adipic acid solutions near and above saturation. We use the steady state and time resolved fluorescence responses of the probe molecule 1-pyrenecarboxylic acid to elucidate information on pre-crystalline adipic acid aggregates in solution. We have used this probe molecule to ensure the proximity of the fluorescent moiety to the solution phase aggregation events of interest. Steady state fluorescence data demonstrate the pH-dependence of the chromophore response, with an acid dissociation constant of $K_a = 1.64 \times 10^{-5}$. The fluorescence lifetime of protonated 1-pyrenecarboxylic acid (HPCA) exhibits a discontinuous change at the saturation concentration of adipic acid, although there is little structural information contained in such data. The rotational diffusion behavior of HPCA reveals the presence of aggregates of adipic acid with the fluorophore. We discuss these data in the context of solute local organization and the limits these data place on the lifetime of the aggregates.

Introduction

There is considerable interest in understanding crystallization from solution from the viewpoint of interactions between individual molecules. In addition to gaining fundamental insight into the poorly understood phenomenon of spontaneous self-assembly from solution, there are significant practical reasons for enhancing our understanding of crystallization. Crystallization is a key unit operation for the purification of compounds during their industrial scale production. On this scale, crystallization is typically accomplished by adjusting bulk solution properties such as solute concentration, solution pH where appropriate, and temperature. Although various methods have been devised to produce crystals having desirable qualities by adjustment of such parameters, these approaches are largely empirical in nature and very little is known about the process of crystallization on a molecular scale. Understanding crystallization in terms of the interactions between individual molecules could lead to the development of on-line monitoring and/or process control schemes for industrial scale crystallization. From a more fundamental perspective, understanding the balance of molecular forces responsible for crystallization could lead to the ability to crystallize complex molecules that are not amenable to crystallization at present.

Previous attempts to detect and describe the nature of solute organization at the onset of crystallization have focused on bulk solution properties.[1-7] Marked changes in solution properties have been seen at the saturation point for several systems studied. Although these results indicated the onset of solute organization, no relationship was established between these changes and any local structure associated with solute aggregation. Berglund has pioneered the use of fluorescent molecules to study changes

in crystallizing systems.[8] These experiments, using the polyfunctional probe molecule pyranine, identified two distinct environments experienced by water molecules in solutions of glucose and that the ratio of the number of water molecules located in each of these environments was shown to be a sensitive indicator of the degree of supersaturation. While these experiments demonstrated the ability to use fluorescent molecules to interrogate solution phase self-assembly phenomena, they were unable to provide a description of crystallization in terms of interactions between solute molecules because the nature of the interaction(s) between the solute and the crystallizing system was not known.

Recent work in our laboratory has demonstrated that molecular scale information on crystallization could be gained through use of "lock and key" probe molecules.[9,10] The principle behind this approach is to use a fluorescent probe molecule as a reporter of its local environment. The probe molecule contains a pendant side group that is similar or identical to the chemical functionality contained in the crystallizing matrix. Because of the structural commonality between the chromophore and the crystallizing matrix, we can interrogate local organization associated with the crystallizing molecules. Experiments using glycosyl resorufin (GR) as a probe molecule in aqueous solutions of glucose have demonstrated its incorporation into the crystallizing matrix as well as the ability of the fluorophore to report local structural information.[10] In a rotational diffusion experiment, for solute molecules that do not interact in a chemically specific manner with their environments, the expected result is that the reorientation time will depend linearly on the viscosity of the medium. Measurement of the rotational diffusion dynamics of GR in glucose solutions yields viscosity-independent reorientation times in the glucose

concentration region near saturation and extending into supersaturation. In contrast, reorientation times for the non-glycosylated native resorufin chromophore were found to agree with those predicted by the variation in solution bulk viscosity. These results indicate that GR acts as a site for solute aggregation. Reorientation times measured for GR compared to that of resorufin demonstrated that GR incorporates selectively into solute aggregates due to presence of the pendant gylcosyl moiety. The reorientation data also revealed that aggregates of glucose forming in solution persist for times on the order of a nanosecond. The investigation of GR incorporation into glucose demonstrate the feasibility of this approach, and it is important to determine its generality on systems that are more amenable to interpretation and at the same time are of greater practical significance.

We have extended the application of "lock and key" probe molecules to systems containing carboxylic acid functionalities. This chapter focuses on the use of the probe molecule 1-pyrenecarboxylic acid to study the pre-crystalline aggregation behavior in aqueous adipic acid solutions (Fig. 2.2). Adipic acid was chosen as a model system due to its significance as one of the major constituents in the production of Nylon-6,6®. More recently, adipic acid has played an important role in helping to eliminate the use of chlorofluorocarbons during the manufacture of solid state electronics.[11] Mild solutions of adipic acid are used instead of conventional rosin flux to remove metal oxides from circuit boards in preparation for soldering. These and other uses of adipic acid contribute to annual global demand for adipic acid of 1.9×10^9 kg.[12]

We report on the steady state and time resolved fluorescence response of PCA in aqueous solutions spanning adipic acid concentrations ranging from sub-saturation to

supersaturation. For all these measurements, the concentration of PCA is fixed at 0.5 ppm, placing it in the regime of a trace impurity. We find that there is a competition between acid/base equilibrium and the complexation of the protonated chromophore with adipic acid. Separating the contributions from each process reveals significant association between PCA and adipic acid in the region of adipic acid saturation. Measurements of fluorescence lifetimes for PCA in adipic acid solutions demonstrate the sensitivity of this probe to changes in solution composition and the onset of solute self-assembly. We have measured rotational diffusion behavior of PCA in adipic acid solutions and our data indicate the onset of solute aggregation occurs well before the saturation concentration. These data indicate the average aggregate size of four adipic acid molecules remains constant into supersaturated concentration regime. The data presented here point collectively to significant pre-crystalline aggregation in solutions that are significantly lower in adipic acid concentration than that required for crystallization. The steady state fluorescence, lifetime and reorientation data are complementary in the sense that all indicate the complexation and extent of deprotonation of the probe molecule, but each technique senses a different aspect of these intermolecular interactions.

Experimental

Chemicals: Adipic acid was obtained from Aldrich (99%) and used as received. All solutions were prepared using HPLC grade water from Mallinckrodt Baker, Inc. 1-Pyrene carboxylic acid (PCA) was purchased from Aldrich (97%) and used without further purification.

Steady State Fluorescence Measurements: Steady state emission spectra were obtained using a Hitachi F-4500 fluorescence spectrophotometer. Determination of the formation constant between PCA and adipic acid was performed using a 2.5 nm band pass for the excitation and emission monochromators.

Time-Correlated Single Photon Counting (TCSPC) Spectrometer: The time correlated single photon counting spectrometer used to measure fluorescence lifetimes and perform rotational diffusion measurements is shown in Figure 2.2. A mode locked CW Nd:YAG laser (Quantronix 416) generates ~ 9 W average power at 1064 nm. Pulses of 1064 nm light are 100 ps FWHM with a repetition rate of 80 MHz. The laser is equipped with a SHG assembly (Quantronix model 324) using an angle tuned Type II KTP crystal to frequency double mode-locked pulses to 532 nm (~600mW). Mirrors then route the output of the Nd:YAG laser to excite a cavity-dumped, synchronously pumped dye laser (Coherent 702-2). The output of the dye laser can be tuned over a broad range of wavelengths with proper choice of optics and dyes. For the work describe in this chapter, pulses of 646 nm (Kiton Red dye, Exciton optics) light are produced at a repetition rate of rate of 4 MHz and are characterized by autocorrelation times that are 5 ps (FWHM). Pulses of light are directed from the dye laser onto a beam splitter with

90% of the intensity directed for excitation of the sample and 10% being directed onto a fiber optic delay loop, which enables a temporal offset between reference and signal pulses to be achieved. The portion of the beam sent for excitation of the sample is focused into a $LiIO_3$ crystal (Type I SHG) and frequency doubled to 323 nm ($\leq$ 1 mW average power). A cylindrical lens is used to re-collimate the beam and compensate for astigmatism and is followed by removal of the fundamental wavelength using a color glass filter (BG-3). The polarization is then rotated to be 0°with respect to the laboratory z-axis (vertical) using a fused silica fresnel rhomb pair (CVI Laser Corporation FRUV-2). The polarized UV excitation is focused into the sample susing an 88 mm focal length bi-convex fused silica lens. Emission is collected in the right angle configuration using a reflective microscope objective (Ealing x36/0.5) and a Glan-Taylor prism to select the observed polarization. A polarization scrambler is then used to randomize the polarization and the emission from the sample is then focused into a subtractive double monochromator (American Holographic DB-10). In order to increase signal throughput, the monochromator was mounted to orient the entrance slit horizontally, at the expense of some time resolution. This configuration ensures maximum overlap between the image formed by the reflective objective and the entrance slit of the monochromator. Lifetime measurements are typically performed by selecting a polarization of 54.7° (magic angle) to prevent contributions to fluorescence decays from molecular motion. Rotational diffusion dynamics measurements are made by observing emission at polarizations of 0° [$I_{\parallel}(t)$] or 90° [$I_{\perp}(t)$]. A Hammamatsu (R3809U-50) microchannel plate (MCPMT) operating at a supply voltage of 3.1 kV was used to detect emission. The reference pulse is detected using an avalanche photodiode detector (PD, Hammamatsu S2381) and this

signal is routed into one channel of a quad constant fraction discriminator (CFD tennelec TC 455) for processing. The output from the reference channel of the CFD is sent to a time-to-amplitude converter (TAC, Tennelec TC864) and serves as the stop for the TAC. The output from the MCP-PMT is sent to a second channel of the CFD for processing and serves as the start signal for the TAC. Configuring the detection electronics in this so-called "reverse" mode ensures operation of the TAC in a linear conversion range. The TAC output counts are displayed using an oscilloscope (Tectronix 2230) and rate meter (Tennelec TC 525), which are then recorded with a multichannel analyzer (MCA, Tennelec PCA-II). Typically, the instrument response function for this system is ~35 ps FWHM while the lifetimes measured ranged from 4 ns to 160 ns. A detailed description of these detection electronics can be found elsewhere.[13] For the work presented in this chapter, emission was monitored at 425 nm using a 10 nm bandpass. The probe molecule was present in all solutions at a concentration of 0.5 ppm. For lifetime and reorientation measurements, the sample cuvette was placed in a temperature-controlled heat sink (brass block) maintained at 293.0 ± 0.5 K (Neslab Endocal). In lifetime experiments, all solutions were subjected to at least three freeze-pump-thaw cycles to remove dissolved oxygen and emission was collected over all polarization angles to avoid contributions to the spectral dynamics due to reorientation of probe molecules. While this method of data collection can, in principle, lead to small deviations from data collected only at the magic angle, we observe exact agreement between the two methods for our experimental conditions.

Data Analysis: Throughout the work described in this thesis the fluorescence lifetimes range from ~ 4ns to ~160 ns while the instrumental response function is ~ 35 ps

FWHM. For this reason the response function was not deconvoluted from the experimental data. Deconvolution of the instrumental response from lifetime and rotational diffusion data can be avoided by fitting exponential decays to data sets beginning where the instrumental response function has decayed to a value ≤ 5% of its maximum intensity. The experimental data were fit to exponential models using the Origin® (Microcal) fitting program

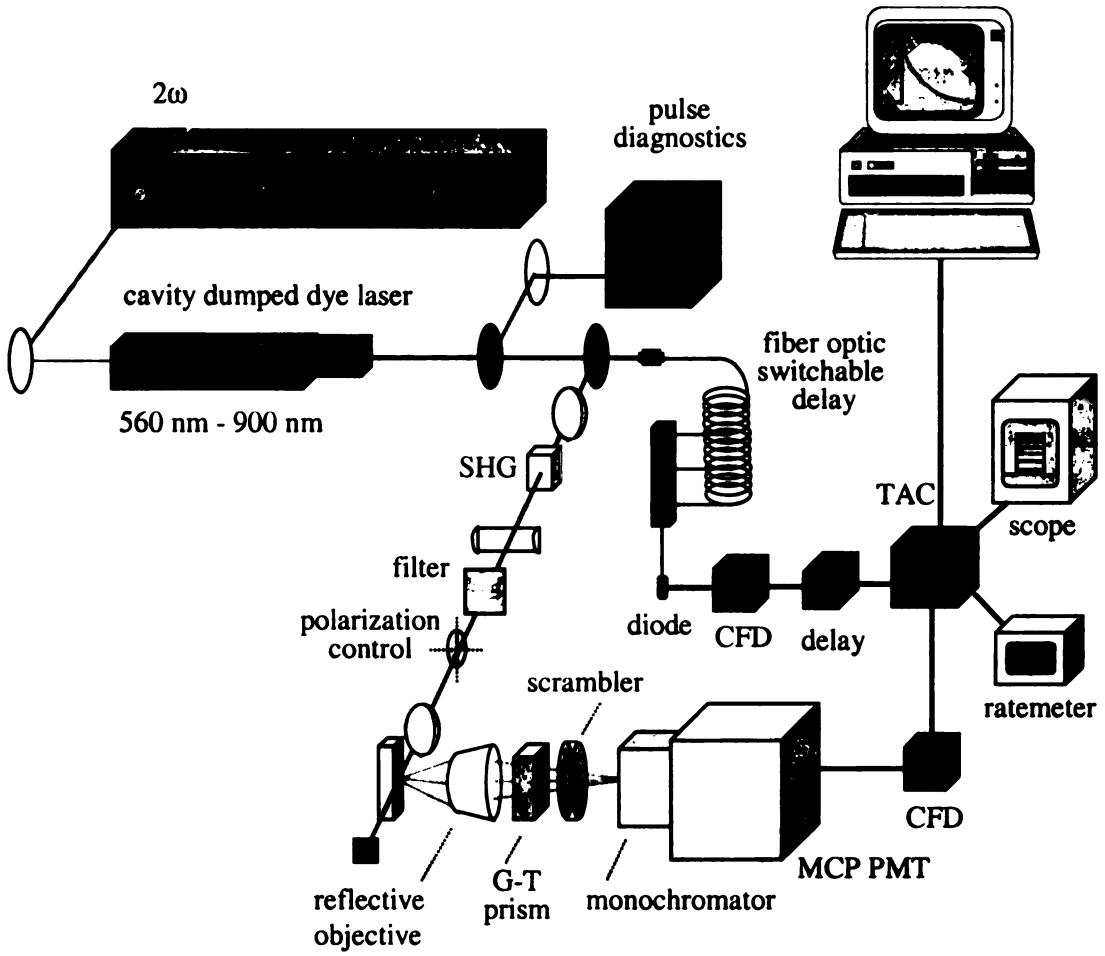

Figure 2.1 Time correlated single photon counting spectrometer used to measure fluorescence lifetimes and rotational diffusion dynamics

Results and Discussion

We have acquired three different bodies of data on the 1-pyrenecarboxylic acid-adipic acid system to gain better insight into the pre-crystallization behavior of adipic acid. Because the different types of data are complementary in nature but do not sense the same phenomena, we consider them individually before discussing the relationships between these different data sets.

We have used aqueous solutions of adipic acid as a model system for understanding crystallization. Adipic acid offers experimental advantages over aqueous glucose solutions used previously. The saturation concentration of adipic acid (1.86% (w/w)[14]) is much lower than that for glucose (55% (w/w)). Solutions of adipic acid, prepared in the range from sub-saturation to supersaturation, differ from pure water in their bulk solution properties to a significantly lower extent than the corresponding glucose solutions. For limited-solubility systems such as adipic acid in water, changes in the probe molecule optical response due to incorporation are distinguished more easily from those due to changes in bulk solution properties.

We consider first our findings on the steady state fluorescence response of the probe molecule. For the sake of clarity we will designate the protonated probe HPCA and the deprotonated form as PCA^-. Our data provide insight into the competition between the acid-base equilibrium of the probe molecule and the propensity of the

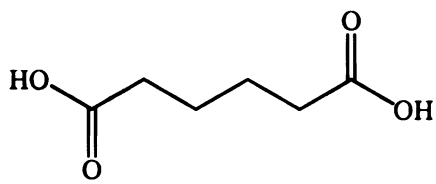

Adipic Acid

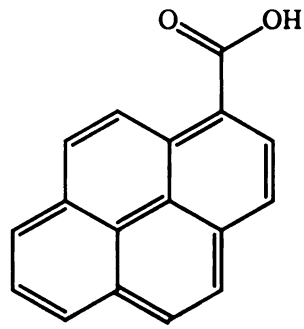

1- Pyrenecarboxylic Acid

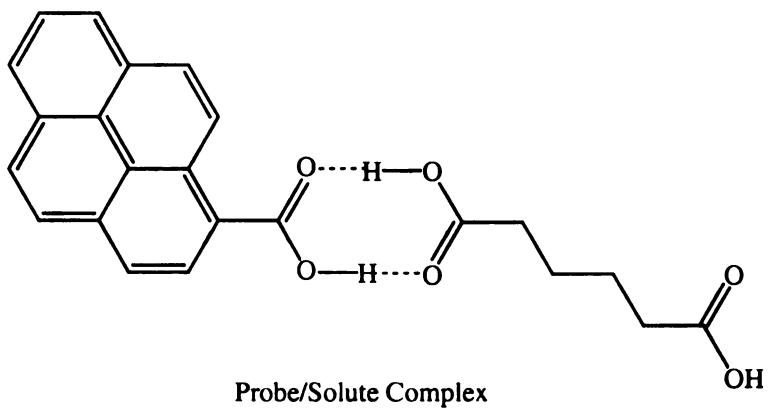

Probe/Solute Complex

Figure 2.2 The structures of 1-pyrenecarboxylic acid (HPCA), adipic acid, and a postulated structure for the complex.

protonated probe to associate with protonated adipic acid solute molecules. We discuss the use of steady state spectra to calculate the acid dissociation and complex formation constants for HPCA and its complex with adipic acid. Data from fluorescence lifetime experiments are presented and we comment on the utility of fluoresce lifetimes in sensing changing solution composition and the onset of solute aggregation. Finally, reorientation times of HPCA in solutions of adipic acid are discussed. Data from dynamical measurements provide a more detailed description of interactions between solute

molecules in solution from which a molecular scale description of pre-crystalline aggregation can be developed.

Steady State Fluorescence: The optical emission response of 1-pyrenecarboxylic acid is very sensitive to the presence of small amounts of adipic acid. Although these spectra do not offer an explicit molecular scale description of solute self-assembly, they are important because they provide insight into the *average* environment sensed by the probe molecule and are sensitive to both complexation and protonation/deprotonation equilibria. These spectra also serve as a spectroscopic guide for the lifetime and reorientation measurements.

The emission spectra of HPCA in adipic acid solutions are shown in Figure 2.3. From these data we note a large change in the band structure between the spectrum taken for the probe molecule in pure water and that taken in a 2.6×10^{-2} M solution corresponding to 20 percent of saturation. While the addition of this much adipic acid will certainly alter the dielectric response of the solution, we observe no measurable change in solution bulk viscosity. The essential question is whether these spectral changes are the result of a pH change in solution associated with the addition of adipic acid or they are reflective of a specific molecular interaction between the probe and adipic acid.

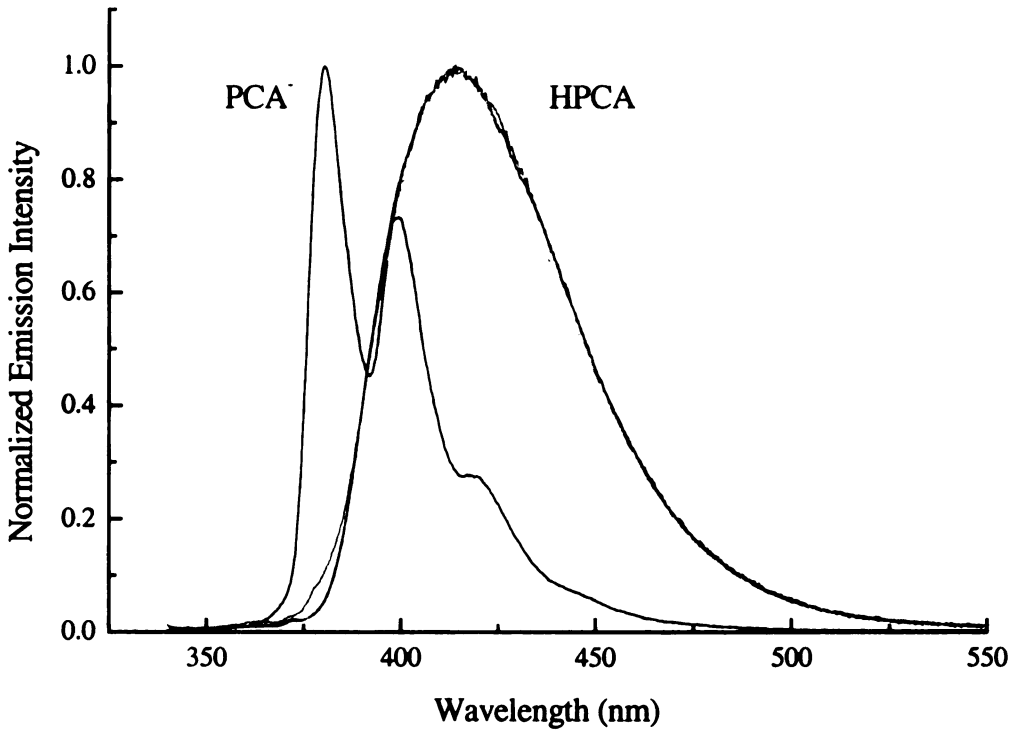

Figure 2.3 Emission spectra of 1-pyrenecarboxylic acid in water and adipic acid solutions. The spectrum of PCA^- contains distinct features at ~375 nm, 400 nm and 420 nm. The broad spectra centered at 418 nm are for HPCA in adipic acid at concentrations between 20% and 110% of saturation.

To evaluate the role of pH on the optical response of the probe, we have measured the emission spectrum as a function of solution pH in buffered solutions and as a function of adipic acid concentration, where the pH is measured for each adipic acid concentration. We have measured the optical response of the probe under these two conditions to elucidate the balance between two competitive reactions,

$$HPCA \underset{}{\overset{K_a}{\rightleftharpoons}} PCA^- + H^+ \qquad K_a = \frac{[H^+][PCA^-]}{[HPCA]} \qquad [2.1]$$

$$\text{HPCA} + \text{AA} \underset{}{\overset{K_c}{\rightleftharpoons}} \{\text{HPCA-AA}\} \qquad K_c = \frac{[\{HPCA - AA\}]}{[HPCA][AA]} \qquad [2.2]$$

In these equations we consider that only the protonated form HPCA can complex with the adipic acid solute and that the dominant form of adipic acid in the pH range we use is the doubly protonated form. We will return to a discussion of these points later.

We consider the buffer solution measurements first because they allow for the determination of K_a separately from K_c. The acid dissociation constant for the HPCA/PCA$^-$ equilibrium was recovered by measuring steady state spectra of buffered solutions containing measurable amounts of both HPCA and PCA$^-$. Each form of the probe contributes to the overall fluorescence intensity in proportion to its concentration.

$$F = \Lambda c \qquad [2.3]$$

In this way the total fluorescence intensity from a sample measured at a given wavelength will be the sum of contributions from both the free and complexed forms:

$$F_{\lambda_i} = \Lambda_{\lambda_i}^{HPCA}[HPCA] + \Lambda_{\lambda_i}^{PCA^-}[PCA^-] \qquad [2.4]$$

Where Λ is the proportionality constant relating fluorescence and concentration for each form at a given wavelength. Fig. 2.4 shows calibration plots of fluorescence intensity versus concentration for each species at 390 nm and 418 nm. We recover the proportionality constant Λ for each species by taking the slope of each plot. Knowing Λ at these wavelengths for each form, we measure the fluorescence intensity at two separate wavelengths and calculate the concentrations of each species by solving simultaneous equations having the form of Eq. 2.4 From these measurements in buffer solutions spanning the range of 3.4 to 4.7, we recover $K_a = 1.64 \times 10^{-5}$.

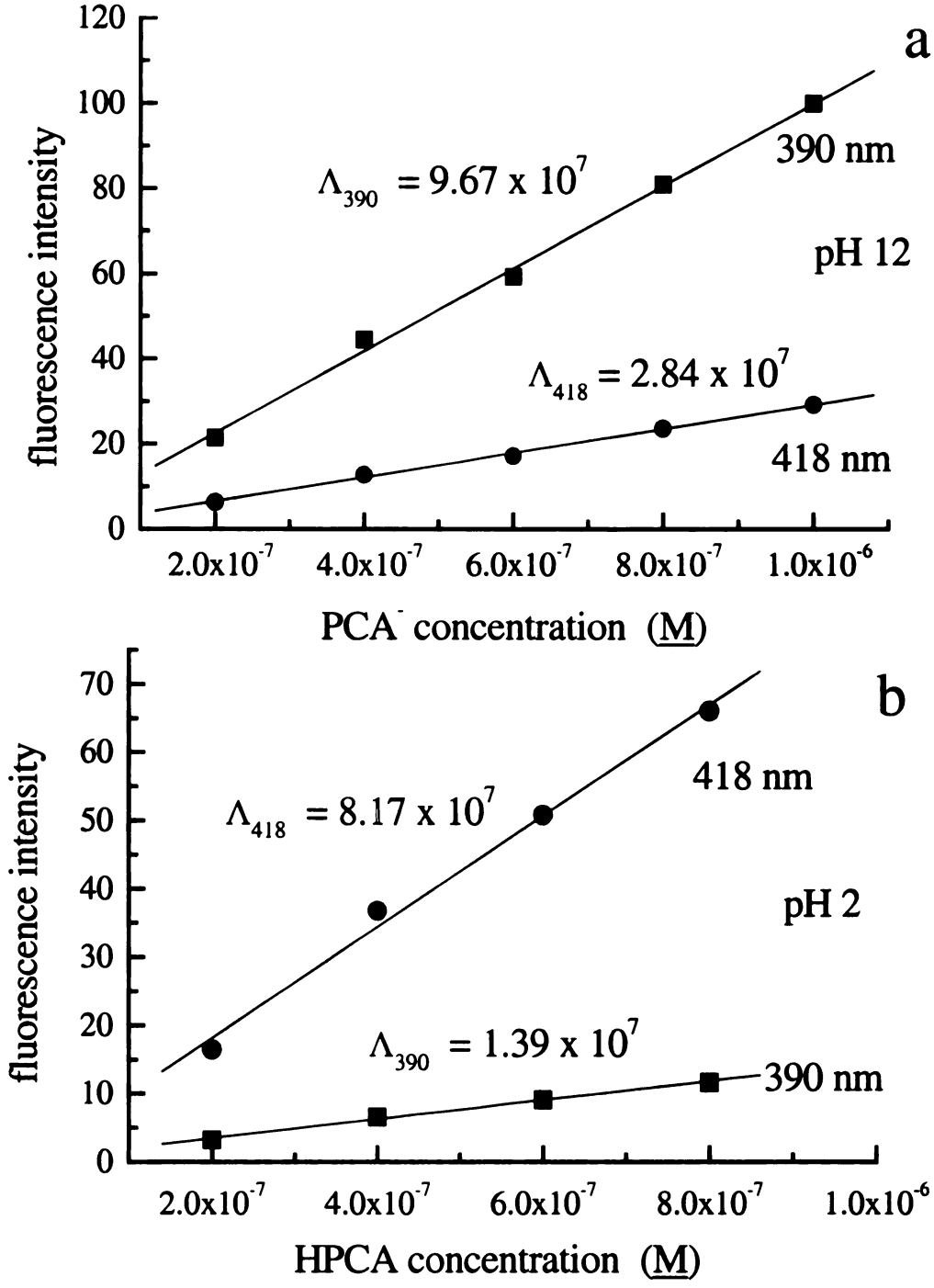

Figure 2.4 Emission intensity calibration curves for emission at 380 and 418nm. (a) Relationship between PCA^- concentration and emission intensity, taken at pH 12 (b) Relationship between HPCA concentration and emission intensity, taken at pH 2.

When measurements analogous to those described above are made using adipic acid to control the pH, the value of the recovered equilibrium constant varies in a systematic manner that is proportional to adipic acid concentration. We understand this behavior in the context of there being competition for HPCA in adipic acid solutions (see Eqs. 2.1 and 2.2). With the value of K_a determined, we can solve iteratively for the value of K_c. The only quantity that we cannot determine directly is [{HPCA-AA}] because the emission response of the complex is overlapped with that of the free protonated form, HPCA. The initial approximation we extract from these spectral data can be used to solve the relevant equilibrium expression numerically. Iterative calculations, including competition with acid/base equilibria can be done according to the formula

$$K_c = \frac{K_a\left(C_{PCA} - [PCA^-] - [HPCA]\right)}{[H^+]C_{AA}[PCA^-]} \qquad [2.5]$$

Eq.2.5 is derived from Eqs. 2.1 and 2.2 and the mass balance for the system. In Eq. 2.5, C_{PCA} is the analytical concentration of the probe molecule, [PCA^-] is the concentration of the dissociated form, determined spectroscopically, [HPCA] is the concentration of the protonated form determined spectroscopically and C_{AA} is the analytical concentration of adipic acid. We have used C_{AA} because HPCA can complex with both HAA^- and H_2AA and in the pH range of the measurements we report here, all of the adipic acid is in one of these forms.[15] The iteration we perform to achieve a convergent value of K_c is based on the fact that we measure spectroscopically the sum of the complex and protonated forms. Initially we assume all of the spectroscopic response is from HPCA and determine K_c. From K_c we calculate [{HPCA-AA}]/[HPCA] according to Eq. 2.2 and use this ratio to estimate the actual concentration of HPCA.

Convergence is achieved typically in three iterations. We obtain a value of $K_c = 150 \pm 40$ $\underline{M}^{-1}$. While this is a modest formation constant, because of the adipic acid concentrations we use and the pH range we work in, complexation plays an important role in our measurements.

We turn next to the nature of the complex. There is ample literature precedent for the formation of carboxylic acid ring bound dimers in solution through hydrogen bonding between their functional groups.[16] Such a complex necessarily requires that both carboxylic acid moieties be protonated. Our reorientation data (*vide infra*) demonstrate clearly the presence of probe-solute complexes in solution.

We recognize that there are limitations to this treatment. Not all HPCA will complex in a 1:1 ratio with adipic acid. HPCA may also complex in a 2:1 ratio with adipic acid or in a 1:1 ratio with itself. We consider each of these complexes to be negligible due to the enormous stoichiometric excess of adipic acid and low concentration of HPCA. It should also be noted that formation of adipic acid oligomers as well as equilibria between protonated forms of adipic acid serves to lower the concentration of adipic acid available for complexation with PCA. Failure to account for these competing equilibria will result in calculated values of K_c being lower than the true value. We consider the value of K_c we determine experimentally to represent a lower bound. We need also to consider the value of K_c for the HPCA-adipic acid complex relative to that determined for other similar systems. The K_c for acetic acid dimerization in water has been measured to be 0.01 $\underline{M}^{-1}$ and for acetic acid dimerization in chloroform $K_c = 4 \times 10^3$ $\underline{M}^{-1}$.[17] We consider these values to be in good agreement with our value given the chemical differences in the systems for which there are data available. With the

establishment of substantial complexation between PCA and adipic acid, we consider next the information available from time domain measurements.

Lifetime Measurements: The existence of solution phase complexes between HPCA and adipic acid demonstrates environmental heterogeneity on a molecular length scale. However, the steady state spectra are insensitive to changes in probe molecule complexation and acid-base equilibria beyond 20 percent of the saturation concentration of adipic acid. Because of the limitation in dynamic range and information content of the steady state measurements, we consider the time domain response of HPCA in adipic acid.

We report fluorescence lifetimes for HPCA in pure water and solutions of adipic acid in Fig. 2.5. The decay time constants we report are best-fit values to a single exponential decay using the instrumental response function as time zero. The quality of the fit to the data was evaluated on the basis of plots of the residuals. For all of the time constants we report, the residuals of the fit were centered about zero throughout the entire region fitted. Because the lifetimes we measure are much longer that the instrument response function, deconvolution did not alter the fitted parameters. The error bars shown represent the uncertainty in each measurement reported to the 95% confidence limit from at least nine individual determinations. As noted above, for all lifetime measurements, oxygen was removed from the solutions using at least three freeze-pump-thaw cycles. We find that the fluorescence lifetime of PCA is much less sensitive to the presence of oxygen than its parent chromophore, pyrene.[18]

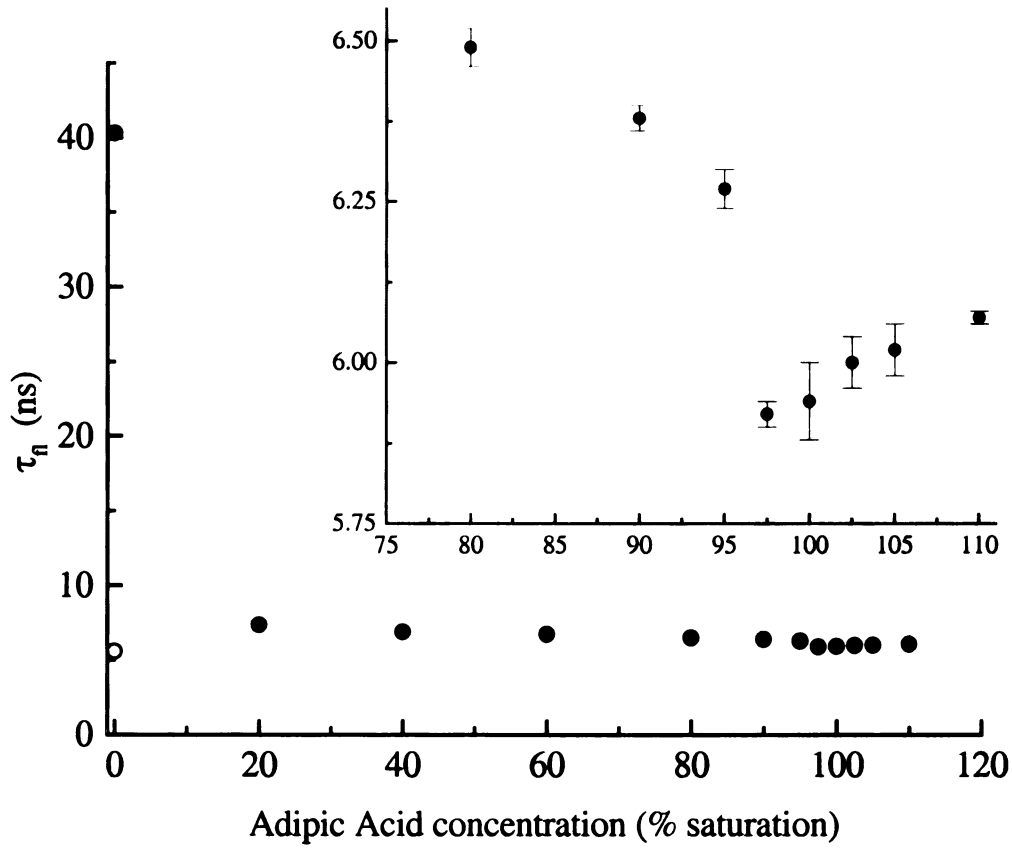

Figure 2.5 Dependence of chromophore fluorescence lifetime on adipic acid concentration. The data points for pure water are for PCA$^-$ (•, 40 ns) and HPCA (o, 5.65 ns). For solutions containing adipic acid, the dominant chromophore is HPCA. Lifetimes were recorded collecting emission at 425nm. For all of these data the uncertainties are within the point presented on the plot. Inset: Expanded region showing discontinuity in HPCA lifetime near saturation concentration.

We note several interesting features in these data. First, going from pure water to 20 percent of adipic acid saturation produces a marked decrease in fluorescence lifetime. The onset of this decrease correlates with our findings from steady-state measurements. This decrease in lifetime is associated with the change in the dominant form of the chromophore going from dissociated PCA$^-$ in water to protonated and partially

complexed HPCA. We calculate that at 20% of saturation, the ratio of complexed to free HPCA is 3.9:1. The lifetime of the protonated form in water (pH 2) is also presented in Fig. 2.5. The second feature of interest appears near saturation for adipic acid. The inset to Fig. 2.5 shows an expanded view of the data in the region between 80 and 110 percent of adipic acid saturation. These data show a clear discontinuity in the trend of fluorescence lifetimes measured near saturation. The decrease in fluorescence lifetime observed between 95 and 97.5 percent of saturation is much larger than between 90 and 95 percent of saturation indicating this discontinuity cannot be attributed to a change in bulk solution composition. We believe that this anomalous behavior is the result of a substantial change in the local environment experienced by the probe molecule. We hesitate to assign this anomaly to any change in aggregation because such an explanation is not supported by rotational diffusion measurements (*vide infra*). While it may be tempting to argue for anomalous behavior of the solution dielectric response near saturation, the relationship between the dielectric response of the medium and the fluorescence lifetime of the chromophore is not clear and depends on assumptions about the nature of the coupling between the solvent and solute. Because we do not have any explicit information that bears on the strength or functionality of this coupling, we will not speculate on the relationship between solution dielectric response and fluorescence lifetime.

At this point it is important to consider that we do not observe the anomalous discontinuity in lifetime at the expected saturation concentration and we cannot account for this deviation in the context of solute impurity because such an explanation would cause a deviation to concentrations higher than the expected saturation concentration. It

is crucial to note, however, that we have not corrected for activity and, while a deviation opposite from that seen may be expected, given the complexity of the system, it is not possible to determine, *a priori*, in which direction we would expect the most significant deviation. We believe that the chromophore is sensing solution activity and not concentration, and thus the appearance of the anomaly at a concentration slightly different than the expected saturation concentration is reflective of the non-ideal behavior of the adipic acid solution. We note that, because of the sensitivity of fluorescence lifetime measurements to the concentration of adipic acid, it is possible, in principle, to use this technique as a diagnostic for proximity to saturation.

The key point from the lifetime measurements is that they reveal the presence of some undefined local organization that is responsible for the observed anomaly at or near saturation. The details of this behavior are not well understood and we turn next to rotational diffusion measurements because information from these measurements can provide further insight into local organization in this complex system.

Reorientation Dynamics: The data presented thus far indicate that HPCA exhibits a substantial affinity for adipic acid, validating our assertion that the probe molecules in solution are located in an environment where they will be sensitive to any pre-crystalline aggregation that may occur. In addition, crystals of adipic acid grown in the presence of 0.5 ppm HPCA, when washed to remove probe molecules that may be adsorbed to the crystal surface, can be re-dissolved and exhibit the emission spectrum of HPCA clearly demonstrating incorporation of probe molecules into the crystallizing matrix. Lifetime measurements suggest that, due to association of the solute with probe molecules, changes in the optical response of the probe near saturation can be correlated to events of

solute self-assembly. These results, while important and interesting, do not provide a description of crystallization in terms of interactions between solute molecules. In order to gain this level of insight we have measured molecular reorientation times for PCA^- and HPCA in pure water and aqueous adipic acid solutions. Reorientation dynamics offer substantial insight into the interactions between a fluorophore and its environment. The theory of rotational diffusion measurements has been developed for cases where there is no specific intermolecular interactions between solvent and solute[19] and in cases where there is such an interaction, deviations of the experimental data from theoretical predictions are informative in revealing the nature of the intermolecular interactions. We use this information here to investigate the nature of the interactions between PCA and adipic acid that lead to the formation of aggregates in pre-crystalline environments.

Rotational diffusion is a well developed measurement technique and there is a mature theoretical framework for the interpretation of the data.[19-26] Most of these theoretical treatments are based on the assumption of a continuum solvent as embodied in the modified Debye-Stokes-Einstein (DSE) equation,

$$\tau_{OR} = \frac{\eta V f}{k_B T S} \qquad [2.6]$$

This model relates the orientational relaxation time of a molecule in solution depends on the solution bulk viscosity, η, the solute hydrodynamic volume, V, the Boltzmann constant, k_B, and the solution temperature, T. The interaction between the solvent and solute is parameterized by a frictional term f 27[27,28] and a shape factor S[29] to account for the non-spherical shape of the volume swept out by the reorienting solute. Despite the limitations of this model associated with the assumptions about the nature of the solvent and the parameterization of the solvent-solute interactions, the modified DSE model does

a surprisingly good job of accounting for the rotational diffusion of many solute molecules. While there is relatively little chemical information contained in the measurement of an individual system, a detailed description of solution phase interactions between molecules can be gained by examination of reorientation times when the solution composition is varied in a regular manner.

Experimentally, the reorientation behavior is determined from TCSPC data by construction of the induced orientational anisotropy function R(t) from the signal intensities for emission polarized parallel and perpendicular to the excitation light source,

$$R(t) = \frac{I_{\parallel}(t) - I_{\perp}(t)}{I_{\parallel}(t) + 2I_{\perp}(t)} \qquad [2.7]$$

R(t) can contain up to five exponential decays depending on the rotor shape describing solute motion and the angle between excitation and emission transition moments (δ) of the solute.[30] Despite this potential complexity, the most common form of R(t) is a single exponential decay,

$$R(t) = R(0)\exp(-t/\tau_{OR}) \qquad [2.8]$$

where the physical significance of the quantity τ_{OR} depends on the rotor shape and the orientation of the transition moments. While the functionality of the decay of R(t) offers insight into the dynamics of the molecule, the zero-time anisotropy, R(0) provides information on the spectroscopic properties of the solute. R(0) is related to the transition moment angle δ according to[31]

$$R(0) = 0.4P_2(\cos\delta) \qquad [2.9]$$

where P_2 is the second order Legendre polynomial. The determination of R(0) is a significant concern for reorientation measurements because variations in R(0) for a solute

as a function of solution conditions can cause subtle changes in the form and information content of the decay in R(t). For systems where R(0) remains essentially constant over a range of experimental conditions, the quantities τ_{OR} can be compared to one another directly.[32]

The R(0) and τ_{OR} data for HPCA in adipic acid solutions are presented in Table 2.1. It is interesting to note the difference in R(0) values between HPCA and the native chromophore pyrene. Pyrene exhibits a negative zero-time anisotropy that is characteristic of the angle δ being greater than 54.7°. This angle is not usually found to be 90° because of the strong vibronic coupling that is responsible for many of the features seen in the pyrene emission spectrum.[18] In contrast, 1-pyrenecarboxylic acid exhibits a positive zero-time anisotropy for all solutions measured. The values we report in Table 2.1 correspond to an angle between transition moments of $\delta \sim 40°$. We interpret these data as indicative of the important role that the carboxylic acid functionality plays in mediating the vibronic coupling between the S_1 and S_2 states of the pyrene chromophore. The presence of functionality at the 1- position of the pyrene chromophore can alter the vibronic coupling seen in pyrene, with the effect being greater for substituents conjugated to the ring structure than for those where there does not exist such conjugation. This effect can have important consequences on the observed functional form of R(t) and we will discuss this point in detail in a forthcoming paper.[33]

The data that provide the most information on the behavior of HPCA are the reorientation times as a function of adipic acid concentration. We present these data in Figure 2.6.

Table 2.1 Fluorescence lifetime and rotational diffusion time data for 1-pyrenecarboxylic acid in water and adipic acid solutions

Adipic acid concentration		Fluorescence lifetime	Rotational diffusion	
% Saturation	M	(ns)	R(0)	τ_{OR} (ps)
0	0	40.0 ± 0.1 (PCA^-)	0.13 ± 0.05	90 ±25 (PCA^-)
		5.65 ± 0.05 (HPCA)	0.18 ± 0.04	95 ± 18 (HPCA)
20	0.025	7.37 ± 0.02	0.14 ± 0.02	138 ± 19
40	0.051	6.90 ± 0.01	0.15 ± 0.02	126 ± 12
60	0.076	6.72 ± 0.01	0.18 ± 0.01	119 ± 12
80	0.102	6.49 ± 0.01	0.17 ± 0.01	119 ± 11
90	0.115	6.38 ± 0.01	0.15 ± 0.01	153 ± 19
95	0.121	6.27 ± 0.03	0.17 ± 0.01	146 ± 8
97.5	0.124	5.92 ± 0.02	0.16± 0.01	160 ± 24
100	0.127	5.94 ± 0.06	0.16± 0.02	157 ± 25
102.5	0.130	6.00 ± 0.04	0.19 ± 0.01	142 ± 14
105	0.134	6.02 ± 0.04	0.17 ± 0.01	151 ± 18
110	0.140	6.07 ± 0.01	0.17 ± 0.01	155 ± 13

We note three distinct regions in the reorientation times, with no clear change or discontinuity at the saturation concentration. In addition to the concentration-dependence of HPCA reorientation in adipic acid solutions, we compare the behavior of the protonated and deprotonated forms of the chromophore in water. The reorientation of both forms of the chromophore in water is consistent with the predictions of Eq. 2.6 (*vide infra*). Both the reorientation time constant and the zero time anisotropy are the same for HPCA and PCA^- in water. This finding is somewhat surprising in the sense that the usual result for reorientation of anionic species in solution is that they are slower than the corresponding neutral molecule. The reorientation dynamics of both forms are accounted for by the modified DSE equation in the stick limit. The fact that the reorientation times are the same suggests that for PCA^-, the negative charge is substantially delocalized over the chromophore π system, precluding strong, site-specific interactions with the surrounding solvent. Understanding the origin of this interesting feature in the data requires further investigation. It is important to consider that dielectric friction can, in principle, play a role in determining reorientation times for polar molecules in solution.[34,35] Dielectric friction is most significant in cases where solute molecule is either charged or possesses a large permanent dipole moment in the state interrogated spectroscopically. Semi-empirical calculations[36] indicate that PCA^- has a permanent dipole moment of 14 D in the S_1, and while this seems to be unreasonably large for such a molecule, if we assume this "worst case" value, dielectric friction contributes an additional 1.5 ps to the rotational diffusion time of PCA^-. This increase is unresolvable given the uncertainty in our measurements.

The data in the adipic acid concentration range of 20 to 80% of saturation are essentially constant with a noticeable discontinuity at ~90% of saturation. The reorientation behavior in the 90 to 110% of saturation concentration range are constant.

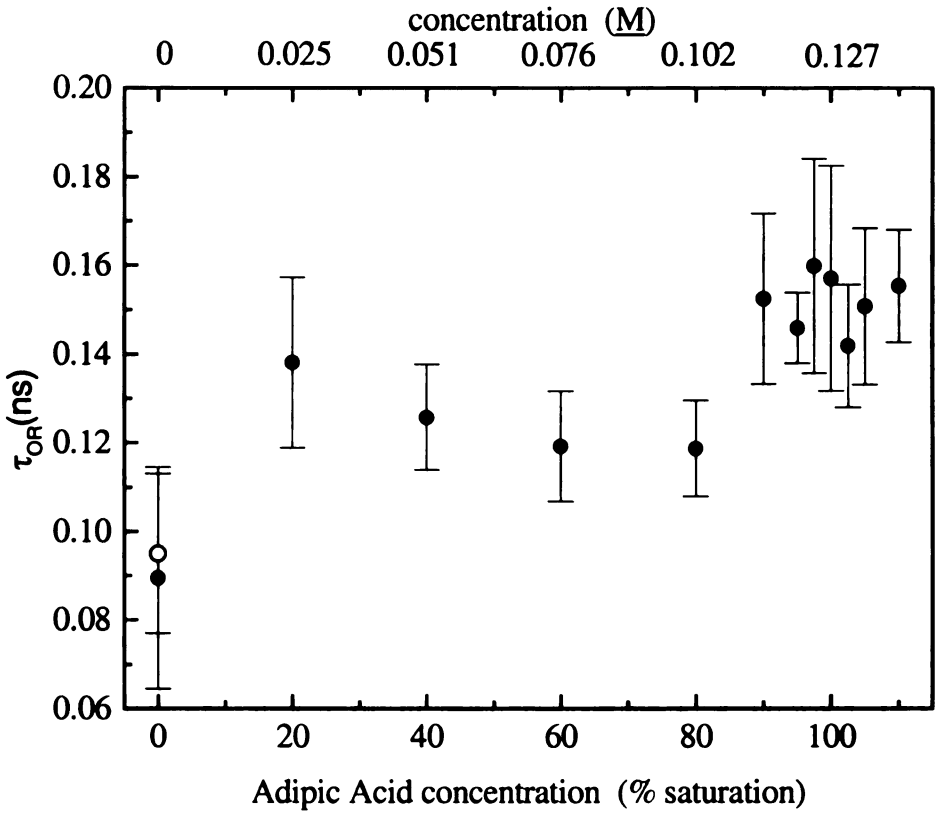

Figure 2.6 Reorientation time as a function of adipic acid concentration. In pure water, the reorientation time of HPCA is presented as an open circle and for PCA- as a solid circle. For all other data points, the dominant chromophore form is HPCA. See text for a discussion.

This stepwise increase in reorientation times for different concentration ranges is not an expected result and provides significant insight into the behavior of the system. While it may be possible to invoke a variety of complex models to account for these data, we choose to use the simplest explanation consistent with the results. The modified DSE

equation can account for these data if the hydrodynamic volume of the reorienting moiety is taken as a variable quantity. Consistent with Eq. 2.6, for isothermal conditions, changes in the measured reorientation time can arise from changes in one of three parameters. These are the solution bulk viscosity, η, the strength of frictional contributions to the solvent-solute boundary condition, f, or changes in the volume and/or shape represented by the terms V and S. Reorientation times scale linearly with the solution bulk viscosity and this quantity can be determined experimentally. We have measured the viscosity of adipic acid solutions at 110% of saturation (η = 1.0 cP) in comparison to that of pure water (η = 0.89 cP) at 25°C. Given the uncertainty in the experimental data, it is unlikely that we would be able to resolve any viscosity dependence in τ_{OR} over this limited range. Our data point to an explanation other than variations in bulk viscosity. The solutions exhibit an increase in viscosity by a factor of 1.1 while the reorientation times increase by a factor of 1.7 in a discontinuous fashion. It is also possible that a change in frictional interactions between HPCA and its environment might be responsible for increases in rotational times. This interpretation, however, seems unreasonable based on the strength of interaction that we observe between HPCA and adipic acid with the steady state data. The typical case for polar molecules in polar solvents is that reorientation in the "stick"[27] limit is observed (f = 1) and that condition is consistent with our data for HPCA in pure water. The complexation we elucidate using steady state measurements suggests that the interaction between the probe molecule and its immediate environment increases with the addition of adipic acid.

As discussed above, frictional contributions are essentially constant for all solutions studied and for either PCA^- or HPCA, dielectric friction does not contribute

measurably to the experimental reorientation times. We must therefore consider that increases in HPCA reorientation times observed with the addition of adipic acid are a consequence of increases in effective hydrodynamic volume of the reorienting moiety.[37] This interpretation is fully consistent with the complexation of HPCA with adipic acid that we have seen in the steady state data.

To implement variations in the hydrodynamic volume of the reorienting molecule in a chemically realistic way, we consider that HPCA can complex with an adipic acid molecule or an adipic acid dimer, trimer or higher oligomer, depending on the dominant oligomer present in the solution. We present a comparison of the experimental data and the model in Table 2.2. In all cases, HPCA exhibits a single exponential decay functionality of R(t). We note that R(0) is essentially constant, indicating that neither protonation of PCA^- or complexation between HPCA and adipic acid alters the angle between the transition moments, despite the marked difference in their steady state emission responses. The functionality and time constant of R(t) for the chromophore in water is most consistent with HPCA reorienting in the stick limit ($f = 1$) as a prolate rotor with a hydrodynamic volume of 210 $Å^3$ [38] and having a shape factor $S = 0.914$.[29]

For the purposes of our modeling we assume the hydrodynamic volume of an adipic acid molecule is 134 $Å^3$ [38] and that the addition of an adipic acid molecule to the reorienting moiety is manifested primarily as a change in V. We do not attempt to account for associated changes in S because of the many conformational degrees of freedom available to the associated adipic acid molecule. To estimate changes in S associated with complexation would be purely speculative and, in addition, would not alter the basic physical picture we present. Using this model, the reorientation time for

HPCA in water is approximated well by Eq. 2.6, and the data for the adipic acid concentration range between 20% and 80% of saturation are consistent with the addition of one or two adipic acid molecules. Our experimental time resolution does not allow us to differentiate between these possibilities, and this intermediate value may be reflective of the lifetime of the complex relative to its reorientation time. We would expect to recover integer complexant values for the reorienting moiety only in the limit that the effective complex lifetime is greater than or equal to the complex reorientation time.

Table 2.2 Calculated rotational diffusion times for the HPCA complex with adipic acid as a function of the number of added adipic acid molecules to the reorienting moiety.

Adipic acid concentration range	Number of adipic acid molecules	Calculated τ_{OR} (ps)	Average experimental τ_{OR} (ps)
0%	0	56	90 ±30
20%-80%	1	93	127±30
	2	128	
90%-110%	3	165	151±32

For a 1:1 complex we predict a reorientation time of 93 ps and for a 2:1 complex we calculate a reorientation time of 128 ps. The average experimental reorientation time of 127 ± 30 ps over this concentration region may be taken to be indicative of a 2:1 complex, but the uncertainty in our data do not allow for this level of discrimination. We note also that the reorientation times at 20% of saturation appear to be slightly longer than at 80% of saturation, and this subtle trend may indicate changes in the average lifetime of the complex with increasing adipic acid concentration. For solutions in the

90% to 110% of saturation range, the model predicts a reorientation time of 165 ps for a 3:1 adipic acid:HPCA complex and our experimental data reveal τ_{OR} = 151 ± 32 ps. It is possible that our ability to sense only up to a 3:1 complex is mediated by the solubility of higher adipic acid oligomers. It is also possible that adipic acid tetramers are the dominant forms in solution in this concentration range.

The reorientation data combined with the steady state complexation data allow us to estimate the distribution of adipic acid oligomers present in solution over the concentration range we have studied. We consider that, for the adipic acid concentration range we have used to determine the HPCA-AA complex, the stoichiometry is 1:1. We further assume that the complexation constant K_c is valid for the dimerization of adipic acid monomers. We expect that, in general, the formation constant for oligomerization of adipic acid will decrease monotonically with increasing oligomer length. The reorientation data reveal that the dominant oligomer in solution for adipic acid concentrations greater than ~0.11 $\underline{M}$ (85% of saturation) is the tetramer, based on the data indicating the trimer and one HPCA molecule. We assume in this model that HPCA is effectively a substitute for a terminal adipic acid molecule in the formation of oligomers. Thus the observation of an {HPCA-AA_3} complex would indicate AA_4 as the dominant form. From these pieces of data, we thus know that the relevant equilibria are

$$AA + AA \underset{}{\overset{k_1}{\rightleftharpoons}} AA_2 + AA \overset{k_2}{\rightleftharpoons} AA_3 + AA \overset{k_3}{\rightleftharpoons} AA_4$$

From the above discussion, $K_c \cong k_1 = 150\ \underline{M}^{-1}$, $k_3 \sim 10\ \underline{M}^{-1}$ and we assume that k_2 is intermediate between k_1 and k_3. We show in Fig. 2.7 the fraction of each oligomer AA_i as a function of adipic acid concentration. These fractions are in excellent agreement with the rotational diffusion data and explain why our τ_{OR} times in the 20% -80% of

saturation region are fit by HPCA association with either 1 or 2 adipic acid molecules. This result is general to aqueous adipic acid solutions and to the extent that $K_c = k_1$, we can apply these findings to other probe molecules.

There is an apparent step-wise increase in τ_{OR} between 0 and 20% of saturation. The data presented in Fig. 2.7 invite speculation as to the nature of the change in τ_{OR} over this concentration range. We do not have experimental data in this concentration range, but we expect any discontinuous change in τ_{OR} would reflect a change in the dominant oligomer from monomer to dimer. As indicated in Fig. 2.7, this would occur at an adipic acid concentration of K_c^{-1}. We note that, given the uncertainty in the data at 0% and 20% of saturation, it would not be possible to resolve any such change unambiguously.

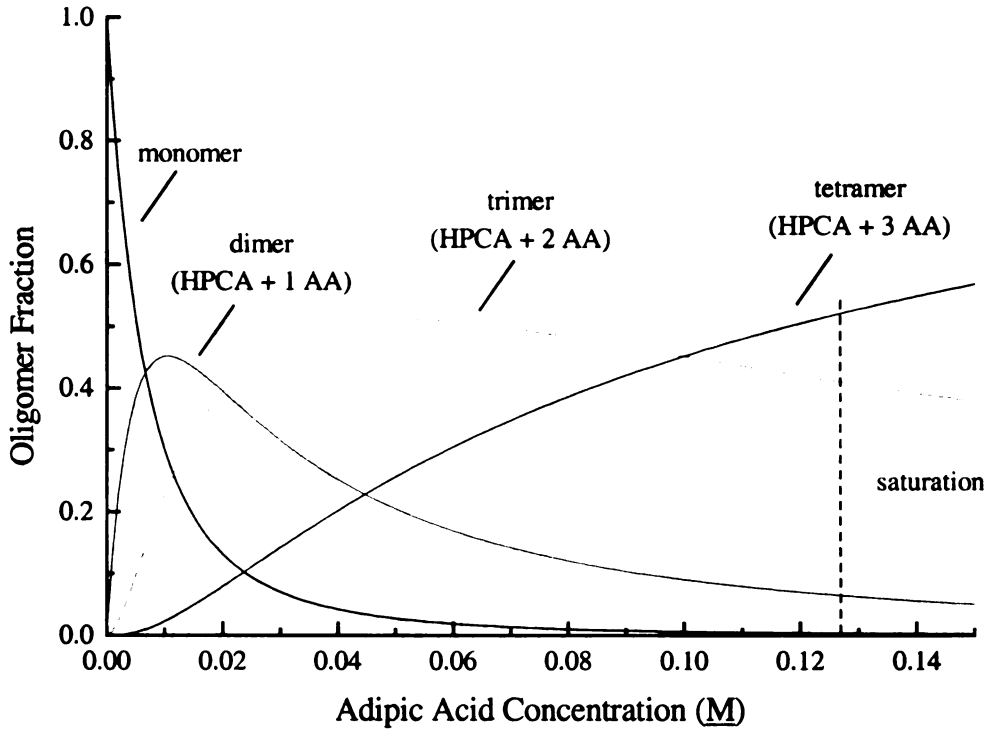

Figure 2.7 Calculated adipic acid oligomer fractions as a function of concentration. Labels indicate the oligomer length for each line.

It is useful to consider the relationships between the various bodies of date we have reported. The steady state data and the fluorescence lifetime data both sense the environment of the chromophore averaged over the lifetime of the excited state. In addition, these measurements are sensitive to changes in structure or complexation at the carboxylic acid functionality conjugated to the pyrene ring system. These bodies of data are correlated to the extent that they are both sensitive to the protonation or deprotonation of the chromophore, but due to inhomogeneity in the emission band, we do not expect a one-to-one correlation of the two bodies of data. The reorientation measurements are

sensitive to local organization and dipolar intermolecular interactions on a timescale given by the rotational diffusion time constant. This time constant is sensitive to the size of the reorienting complex, in contrast to the fluorescence and steady state data and it is not surprising that the lifetime and reorientation data are not outwardly correlated. The reorientation data point to identifiable organization in solution on a time scale of ~100 ps and these same trends are not manifest in data that averages over nanoseconds of time. This comparison places bounds on the lifetime of the aggregates that we sense with the reorientation measurements. These pre-crystalline aggregates have a persistence time that is at least on the order of 100 ps but less than ~5 ns. Given that the longitudinal relaxation time of water, τ_L, is on the order of picoseconds, it is clear that the organization we observe is mediated by the intermolecular interactions between adipic acid and HPCA rather than by the interactions of solvent water with each constituent. Gaining more detailed information on the dynamics of the complexed species will be important in moving these measurements into the realm of being predictive indicators of crystallization.

Conclusions

We have measured the steady state and time resolved fluorescence behavior of HPCA in aqueous adipic acid solutions. The steady state emission data point to the importance of acid-base equilibria for this probe ($K_a = 1.64 \times 10^{-5}$) and the formation of a complex between HPCA and adipic acid with a formation constant of $K_c = 150\ \underline{M}^{-1}$ assuming a 1:1 complex. This assumption is supported by the rotational diffusion data in the adipic acid concentration range where K_c was determined. The time resolved fluorescence data reveal a discontinuous dependence of the lifetime on adipic acid concentration near saturation. While there is limited molecular information available from such measurements, it is possible that this technique can be used as a method for determining the onset of saturation in these solutions. The rotational diffusion data demonstrate the step-wise formation of complexes between HPCA and adipic acid oligomers in solution. The step-wise character of the data is consistent with discrete nature of the complexes. This body of data, taken collectively, serve to bound the lifetime of complexes that form in pre-crystalline systems and indicate that the "lock and key" approach to studying aggregation in pre-crystalline solutions is fully applicable to the family of carboxylic acids. Recent work using related chromophores points to the unique properties of HPCA in sensing complexation.

Literature Cited

1. Myerson, A. S.; Sorrel, L. S.; *AIChE. J.*, **1982**, *28*, 778.

2. Sorrel, L .S.; Myerson, A. S.; *AIChE. J.*, **1982**, *28*, 772.

3. Chang, Y. C.; Myerson, A. S.; *AIChE J.*, **1985**, *31*, 980.

4. Chang, Y. C.; Myerson, A. S.; *AIChE. J.*, **1986**, *32*, 1567.

5. Chang, Y. C.; Myerson, A. S.; *AIChE. J.*, **1986**, *32*, 1747.

6. Larson, M. A.; Garside, J.; *Chem. Eng. Science*, **1986**, *41*, 1285.

7. Larson, M. A.; Garside, J.; *J. Cryst. Growth,* **1986**, *76*, 88.

8. Chakraborty, R.; Berglund, K. A.; *AIChE Symposium Series*, **1991**, *284*, 113.

9. Rasimas, J. P.; Berglund, K. A.; Blanchard, G. J.; *J. Phys. Chem.*, **1996**, *100*, 7220.

10. Rasimas, J. P.; Berglund, K. A.; Blanchard, G. J.; *J. Phys. Chem.*, **1996**, *100*, 17034.

11.. *Electronic News*, **1991**, *38*, 18.

12. Draths, K. M.; Frost, J. W.; *J. Am. Chem. Soc.*, **1994**, *116*, 399.

13. DeWitt, L.; Blanchard, G. J.; LeGoff, E.; Benz, M. E.; Liao, J. H.; Kanatzidis, M. G.

J. Am. Chem. Soc. **1993**. *115*: p. 12158-12164.

14. Mullin, J. W.; *Crystallization*, Butterworth-Heinimann, Oxford, England, 1993.

15. Merck Index, 11th Edition, Merck and Co., Rahway, NJ, 1989, p. 154.

16. Pauling, L.; Brockway, L. O.; *Proc. Nat. Acad. Sci.*, **1934**, *20*, 336.

17. Harris, J. T.; Hobbs, M. G.; *J. Am. Chem. Soc.*, **1954**, *76*, 1419.

18. Karpovich, D. S.; Blanchard, G. J.; *J. Phys. Chem.*, **1995**, *99*, 3951.

19. Debye, P.; *Polar Molecules*, Chemical Catalog Co., New York, 1929, p. 84.

20. Justus, B. L.; Cox, A. J.; Butz, K. W.; Scott, G. W. *Chem. Phys.*, **1988**, *119*, 125.

21. Blanchard, G. J.; *J. Phys. Chem.*, **1989**, *93*, 4315.

22. Quitevis, E. L.; Horng, M-L. *J. Phys. Chem.*, **1990**, *94*, 5684.

23. Dutt, G. B.; Doriswamy, S.; Periasamy, N.; Venkataraman, B. *J. Chem. Phys.*, **1990**, *93*, 8498.

24. Blanchard, G. J. *J. Phys. Chem.*, **1991**, *95*, 5293.

25. Alavi, D. S.; Waldeck, D. H. *J. Phys. Chem.*, **1991**, *95*, 4848.

26. Vauthey, E. *Chem. Phys. Lett.*, **1993**, *216*, 530.

27. Hu, C-M.; Zwanzig, R. *J. Chem. Phys.*, **1974**, *60*, 4354.

28. Youngren, G. K.; Acrivos, A. *J. Chem. Phys.*, **1975**, *63*, 3846.

29. Perrin, F. *J. Phys. Radium*, **1934**, *5*, 497.

30. Chuang, T. J.; Eisenthal, K. B.; *J. Chem. Phys.*, **1972**, *57*, 5094.

31. Fleming, G. R., *Chemical Applications of Ultrafast Spectroscopy*, Oxford University Press, 1986.

32. Blanchard, G. J.; Wirth, M. J.; *J. Chem. Phys.*, **1985**, *82*, 39.

33. Tulock, J. J.; Blanchard, G. J.; *J. Phys. Chem.*, in preparation.

34. Kivelson, D.; Spears, K. G.; *J. Phys. Chem.*, **1985**, *89*, 1999.

35. Kivelson, D.; *J. Chem. Phys.*, **1991**, *95*, 709.

36. Hyperchem V 4.0 using PM3 parameterization.

37. Blanchard, G. J.; *Anal. Chem.*, **1989**, *61*, 2394.

38. Edward, J. T.; *J. Chem. Ed.*, **1970**, *47*, 261.

Chapter 3

The Role of Probe Molecule Structure in Sensing Solution Phase Interactions in Ternary Systems

SUMMARY

We report on the use of 1-pyrenebutyric acid (PBA) as a probe molecule to investigate aggregation phenomena in aqueous adipic acid solutions. Key issues in understanding solution phase aggregation phenomena are the length scale and the persistence time of the aggregates. We have chosen PBA to understand the characteristic length scale and role of probe molecule structure in the examination of solution phase aggregation phenomena. The steady state emission response of PBA in adipic acid solutions yields little information because the carboxylic acid functionality of this probe molecule is not conjugated with the pyrene chromophore. Fluorescence lifetimes for PBA vary in a regular manner in the region of adipic acid saturation, suggesting that the chromophore is not in close spatial proximity to pre-crystalline aggregates that are known to form in these solutions. Rotational diffusion measurements of PBA reveal the presence of adipic acid aggregates in solution but, because of the length of the tether between the chromophore and the carboxylic acid functionality, the ability to resolve distinct intermolecular interactions is limited. This work points to the importance of close coupling between the chromophore and incorporating functionality for such measurements.

Introduction

Achieving an understanding of intermolecular interactions in the solution phase has been an active area of research for at least the past three decades.[1-22] The reason for this activity is that many chemical reactions and separation processes are carried out in solution and achieving predictability over intermolecular interactions would allow for less empiricism in these important areas. To date, the primary approach to the examination of solution phase intermolecular interactions has been to use the transient and/or steady state optical response of chromophores present in low concentration in neat liquids. There have been many models devised to understand data on such systems and one conclusion of this body of work is that the nature of solvent-solute interactions can depend sensitively on the identities of both the solvent and solute molecules.

The probe molecule approach to understanding intermolecular interactions has proven to be useful not only for neat liquids, but also for ternary systems where the third component can be either freely soluble in the solvent or present as a crystallizing moiety. Crystallization is an important industrial process for the separation and purification of many compounds and achieving a molecular understanding of this process could put such efforts on a solid chemical and physical footing. For any ternary system, and for systems that can exhibit spontaneous phase separation in particular, a central issue is the local environment of the probe molecule. Most ternary liquid phase systems are heterogeneous on some length and time scale and the location of the probe molecule relative to these local inhomogeneities determines the information content of the experiment. It has been shown by the Berglund group that, for systems where the probe molecule is structurally distinct from the crystallizing moiety, the probe does not sense pre-crystalline

aggregation effects efficiently.[23] Recent work by the Berglund and Blanchard groups has shown the utility of a "lock-and-key" approach to the study of crystallization, where the optically accessible probe molecule possesses a pendant functionality capable of incorporation into aggregates of the crystallizing moiety.[8-27]

The foci of the work we present here are to understand the role of probe molecule structure in "lock-and-key" investigations of pre-crystalline aggregate formation and to explore the relevant length scale over which the probe is sensitive to solution phase aggregation phenomena. Due to participation in local organization events, certain probe molecules exhibit changes in their optical responses that can be related to associative molecular interactions preceding crystallization. Recent work in our laboratories has demonstrated the utility of lock-and-key probes for interrogation of molecular interactions within different chemical systems.[27] Glycosyl resorufin[26] and 1-pyrenecarboxylic acid (PCA)[27] have been used to probe solution phase aggregation in aqueous glucose and adipic acid solutions, respectively. Studies of both systems demonstrate selective incorporation of the probe molecules into pre-crystalline aggregates and the ability of those probe molecules to provide structural information on the aggregates. Measurement of adipic acid solution phase aggregation using PCA as a probe have yielded considerable structural information, showing stepwise formation of solute oligomers with increasing adipic acid concentration. In that work, the probe molecule is in close spatial proximity to the adipic acid aggregates and thus the sensitivity of the probe optical response to solution phase local organization is high. Results from those experiments have raised a number of fundamental issues, such as the effect of probe molecule structure and the proximity of the chromophore to the

aggregation event. To address these issues, we have measured steady-state and time-resolved optical properties of a similar probe molecule, 1-pyrenebutryic acid (PBA, Fig. 3.1), in aqueous adipic acid solutions spanning concentrations from subsaturation to supersaturation.

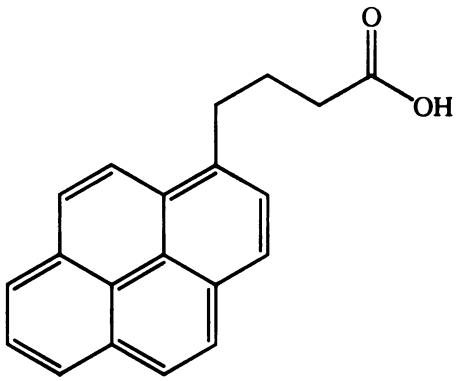

1-pyrenebutyric acid (PBA)

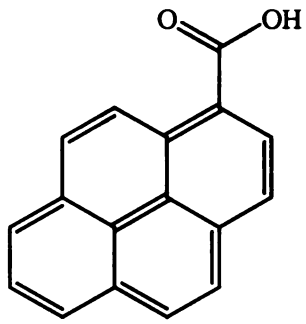

1-pyrenecarboxylic acid (PCA)

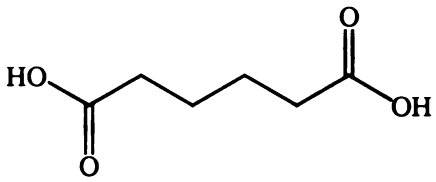

adipic acid

Figure 3.1 Structures of 1-pyrenecarboxylic acid (HPCA), 1-pyrenebutyric acid (HPBA), and adipic acid.

By changing the spacing between the functionalities in the probe molecule responsible for incorporation and optical response, we hope to elucidate the significance of chromophore proximity in reporting aggregation phenomena. For our experiments, PBA is present at the level of trace impurity (0.5 ppm, ~10^{-7} M), a concentration low enough to

likely avoid perturbations to the aqueous adipic acid system. The steady state emission spectra of PBA sense its local environment averaged over the fluorescence lifetime and we find the emission spectrum of this molecule to be largely independent of the protonation status of its carboxylic acid functionality and of changes in solution adipic acid concentration. The time domain response of PBA is sensitive to adipic acid concentration but we do not observe any discontinuous changes in lifetime with the onset of solute aggregation.[27] Measurement of the rotational diffusion dynamics of PBA in these systems provides insight into adipic acid self-association and, when compared to the response of 1-pyrenecarboxylic acid (PCA), sheds light on the length scale over which the probe chromophore is sensitive to local organization about its side group functionality. The key piece of information gained from this work is that the persistence length of solution-phase aggregation phenomena appears to be shorter than the C_4 tether between the incorporating functionality and the chromophore, despite the fact that adipic acid is a C_6 dicarboxylic acid. While the relative insensitivity of the probe molecule PBA to local organization would not be a surprising result for large systems such as biological membranes, it is not clear that this same intuitive understanding would apply to highly dynamic solution phase systems. Our data make this connection.

Experimental Section

Chemicals: Adipic acid (99%) was obtained from Aldrich and used as received. All solutions were prepared using Aldrich HPLC grade water. 1-Pyrenebutyric acid (PBA, 97%) was purchased from Aldrich and used without further purification. PBA was judged to be pure by the existence of a single band in thin layer chromatograms generated using several different solvent systems. The fluorescence lifetime of PBA in distilled water exhibited a single exponential decay (*vide infra*).

Steady State Fluorescence Measurements: Steady state emission spectra were obtained using a Hitachi F-4500 fluorescence spectrophotometer using a 5 nm band pass for both excitation and emission monochromators. The concentration of PBA in all solutions was 0.5 ppm (~ 1.0×10^{-7} M). This concentration was sufficiently low to preclude aggregation or self-absorption effects.

Time-Correlated Single Photon Counting (TCSPC) Spectrometer: The time correlated single photon counting spectrometer used to measure fluorescence lifetimes and rotational diffusion time constants has been described chapter 2 and only a brief outline of its salient features is provided here. The light pulses used to excite the sample are generated with a cavity-dumped, synchronously pumped dye laser (Coherent 702-2) excited by the second harmonic output of a CW mode-locked Nd:YAG laser (Quantronix 416). Samples were excited at 323 nm (Kiton Red, Exciton, with Type I $LiIO_3$ SHG). The pulse repetition rate for these measurements was set to 1 MHz. PBA emission was monitored at 390 nm using a 10 nm bandpass. For lifetime and reorientation measurements, the sample cuvette was placed in a temperature-controlled brass block cell

holder maintained at 293.0 ± 0.5 K (Neslab EX-221). For the fluorescence lifetime experiments, all solutions were subjected to at least three freeze-pump-thaw cycles to remove dissolved oxygen and emission was collected over all polarization angles to avoid contributions to the spectral dynamics due to reorientation of probe molecules. While this method of data collection can, in principle, lead to small deviations from data collected only at the magic angle, we observe exact agreement between the two methods for our experimental conditions.[28,29] Rotational diffusion measurements were made by collecting emission at polarizations parallel and perpendicular to the incident (vertical) electric field polarization. Fluorescence depolarization data were recorded using a 5 ns time window with 1024 resolution elements, corresponding to 4.88 ps/element. For each polarization collected, no less than one thousand counts were collected at maximum intensity. Anisotropy decays and fluorescence lifetimes were fit to a single exponential beginning where the instrumental response function had decreased to at least five percent of its maximum value. Typically, the instrument response function for this system is ~35 ps FWHM and the lifetimes measured range from 120 ns to 150 ns. Deconvolution of the response function from the experimental data was not required. For the reorientation measurements, deconvolution of the response function from the parallel and perpendicular polarization data prior to generation of the R(t) function caused no change in the regressed τ_{OR} decay time constants.

Results and Discussion

A central purpose of the work we report here is developing a fundamental understanding of the role of probe molecule structure in relating the details of transient solution phase organization to chromophore optical response. This effort is part of a larger body of work aimed at detecting, characterizing and understanding local organization and spontaneous self-assembly in the solution phase.[25-27] We have used PBA as the probe molecule in this work to understand both the characteristic length scale of solution phase adipic acid aggregation and also to determine the dependence of the pyrene chromophore response on side group identity. We consider these questions in the context of steady state and time-domain fluorescence measurements and rotational diffusion data. We consider each of these bodies of information separately.

Steady State Fluorescence: We have measured the steady state emission response of PBA in solutions of adipic acid ranging in concentration between 20% and 110 % of saturation (saturation concentration = 1.86% w/w, 0.127 M).[30] These solutions range in pH from 3.2 to 2.8 and we expect that the predominant species contributing to these spectra will be the protonated form of PBA (HPBA) in solutions containing adipic acid. In pure water we expect the dominant form to be deprotonated (PBA^-) on the premise that the pK_a of PBA is ~ 4.8. We base this estimate on the pK_a values for alkanoic acids, which fall in the range of 4.75 to 4.9.[31] We observe no differences between spectra recorded for PBA in pure water and solutions of adipic acid (Figure 3.2).

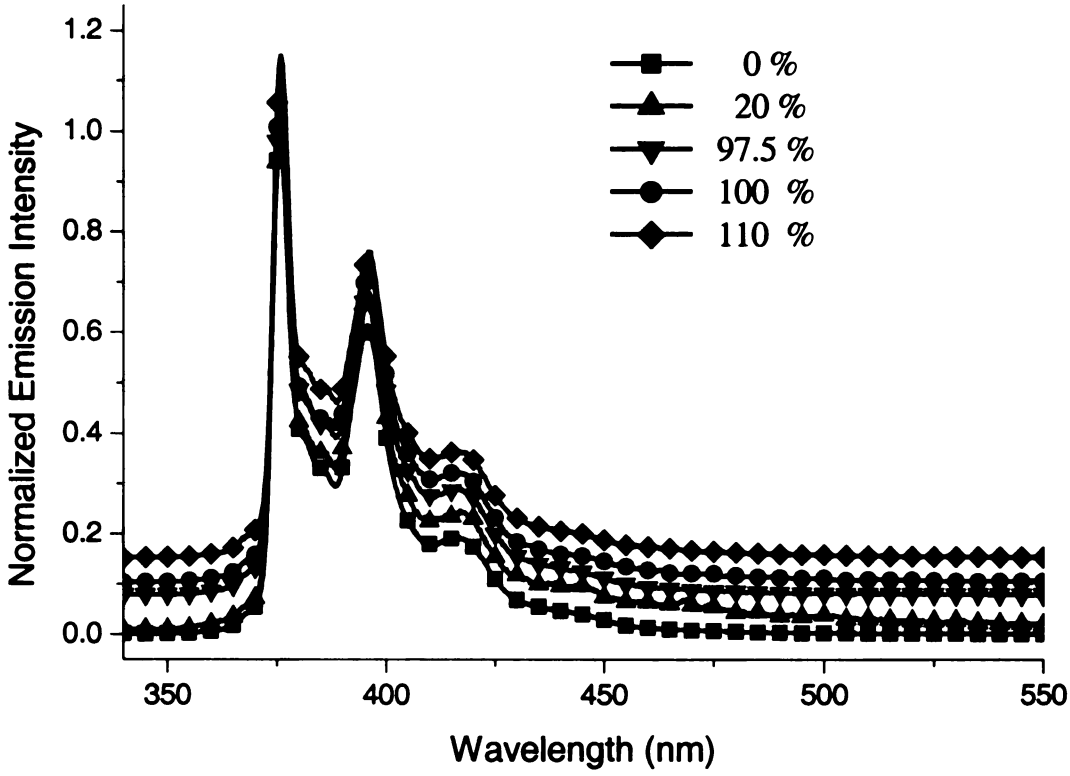

Figure 3.2 Emission spectra of 1-pyrenebutyric acid in water and adipic acid solutions having concentrations between 20% and 110% of saturation. Spectra have been offset for clarity.

Based on this result we conclude that the emission response of the PBA is not significantly sensitive to either the degree of protonation or to the presence of adipic acid. We note that no change in the emission spectral profile of HPBA is seen in the region of adipic acid saturation. This is an expected result given the fact that the PBA carboxylic acid functionality is not conjugated to the pyrene chromophore ring system.

We contrast these results with those obtained using the structurally similar probe 1-pyrenecarboxylic acid (PCA), for which the protonated and deprotonated forms exhibit distinct emission spectra.[27] Differences in the pH-dependent steady state emission spectra of PBA and PCA stem from the proximity of carboxylic acid groups to the pyrene chromophore (Fig. 3.1). For PCA the carboxylic acid group is conjugated with the

chromophore, while for PBA this conjugation is absent. The emission response of PBA is thus insensitive to protonation of the carboxylate moiety. An immediate conclusion of this comparison is that the steady state spectral profile of PCA contains more information on local environment than that of PBA.[27]

The steady state emission data for PBA are important because they underscore the central role of molecular structure in determining the sensitivity of the probe molecule to its local environment. Because of the absence of significant local environmental information in the PBA spectra, we have investigated the time-domain response of this molecule in adipic acid solutions in an attempt to elucidate the effect of chromophore distance from the putative complexation site. Fluorescence lifetime and rotational diffusion dynamics of PBA in adipic acid solution provide subtle but important information on the presence of solution-phase self-assembly in adipic acid solutions.

Lifetime Measurements: We show the fluorescence lifetime of PBA as a function of adipic acid concentration and in buffered solutions in Fig. 3.3. The lifetime data are the average of at least six individual determinations and the error bars represent the uncertainty in the data at the 95% confidence level. The lifetime data exhibit an initial increase in going from pure water to 0.025 M adipic acid (20% of saturation) and we attribute this difference to a change in the predominant species from PBA^- in pure water to HPBA in solutions containing adipic acid. This change in lifetime is in agreement with the lifetime of PBA measured in solutions buffered at pH 12 and pH 2. Despite the absence of a pH-dependence in the frequency domain, there is a clear difference between the protonated and deprotonated forms in the time domain. Over the range of adipic acid concentrations used here, PBA lifetimes exhibit a curvilinear relationship with solution

composition. In comparison, PCA exhibits a discontinuous change in fluorescence lifetime near the saturation concentration and we have related that behavior to the existence of solute local organization.

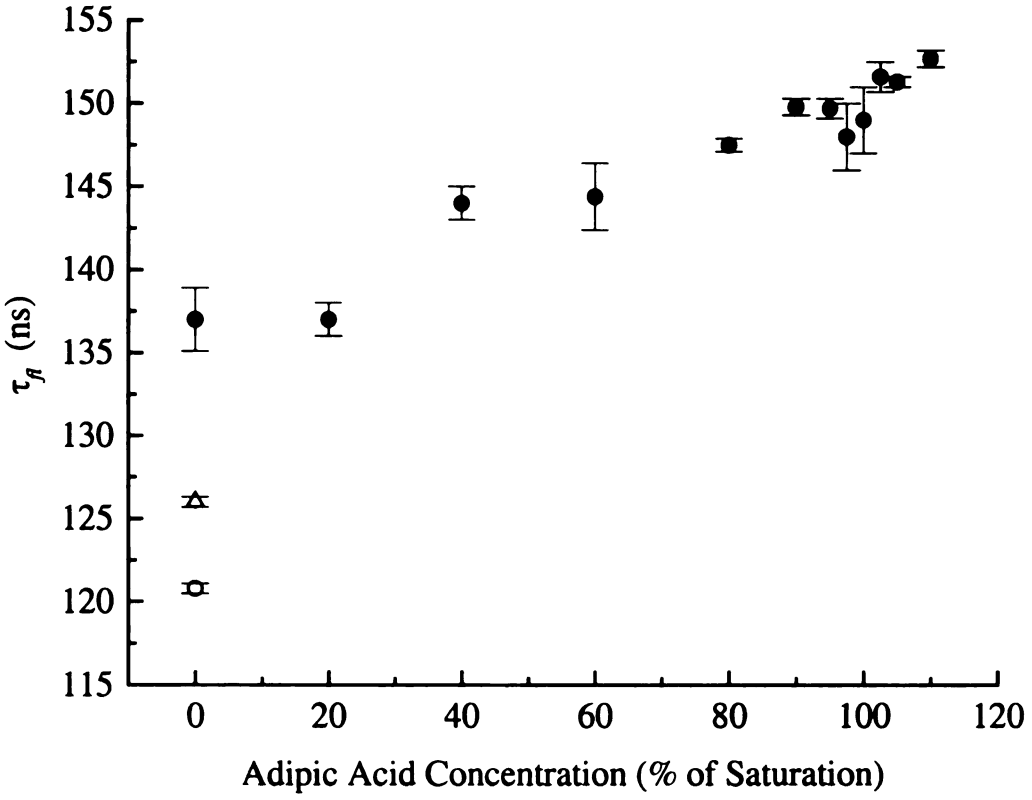

Figure 3.3 The dependence of fluorescence lifetime with solution composition. Open symbols show τ_n of PBA˙ in pure water (○, no buffer; Δ, pH=12). Solid circles show τ_n of HPBA. Error bars show the uncertainty in each data point with 95% confidence intervals.

The form of the local organization is believed to be association with adipic acid as a probe/solute complex hydrogen bonded at their carboxylic acid groups.[27] There is no reason to expect significantly different adipic acid organization here and the absence of an anomalous change in PBA lifetime near saturation suggests that this probe molecule is

relatively insensitive to solution phase self-assembly phenomena because of the distance between the associative complex and the chromophore moiety.

Based on our earlier work with PCA in adipic acid solutions, we expect significant association between protonated PBA and adipic acid. In contrast to PCA, the structure of PBA is such that the steady state emission response is insensitive to the presence of adipic acid oligomers, as we discussed above. The fact that the chromophore and carboxylic acid functionalities are spaced further apart in PBA than in PCA accounts for the difference in the dependence of fluorescent lifetimes with adipic acid concentration for the two molecules. The observation that PBA exhibits no anomalous behavior in τ_{fl} near saturation is consistent with probe-solute association through the carboxylic acid functionality and not by van der Waals interactions between adipic acid and the pyrene ring system. If van der Waals interactions dominated the interactions between the probe molecule and adipic acid, both PCA and PBA would manifest similar lifetime behavior near saturation. We thus expect PBA to sense an environment that is better approximated by bulk solution properties than by local aggregation.

To this point the data we have reported on PBA in adipic acid have demonstrated that this probe molecule possesses limited sensitivity to the presence of adipic acid aggregation phenomena. This limitation arises from the structure of the probe and for two reasons. The active complexation site of PBA is not conjugated to the pyrene chromophore, and that moiety is structurally isolated from the complexation site. Because of this latter structural condition and the relatively long fluorescence lifetime of this chromophore, significant environmental "averaging" mediates the experimental

response and limits its information content. For these reasons we have also examined the rotational diffusion behavior of PBA in these same solutions.

Reorientation Dynamics: Rotational diffusion is a well established technique for the examination of solution phase intermolecular interactions. The basis for the utility of this measurement is the existence of a mature theoretical framework for the interpretation of experimental data.[11,32-38] In most treatments, the starting point is the Debye-Stokes-Einstein (DSE) model, in which the solute is treated as a hard sphere and the solvent as a continuum medium with no discrete molecular properties. Despite the obvious absence of a correspondence between the basic assumptions of this model and real systems, the DSE model has proven to be accurate to within at least a factor of two for most systems studied. Better agreement between experiment and theory can be achieved when the non-spherical shape of the molecule is accounted for[39] and the solvent-solute boundary condition is treated.[40,41] The resulting modified Debye-Stokes-Einstein (DSE) equation is used widely,

$$\tau_{OR} = \frac{\eta V f}{k_B T S} \qquad [3.1]$$

Eq. 3.1 relates the orientational relaxation time constant of a molecule, τ_{OR}, to the solution bulk viscosity, η, the solute hydrodynamic volume, V, the Boltzmann constant, k_B, and the solution temperature, T. The interaction between the solvent and solute is parameterized by a frictional coefficient f [27,28] and a shape factor S [29] to account for the non-spherical shape of the volume swept out by the reorienting molecule. While there is limited chemical information contained in the measurement of an individual system owing to the assumptions involved in determining the quantities η and V and the model-dependence of f and S, examining reorientation in systems where a single chemical

property is varied in a regular manner can provide substantial insight into the nature and strength of intermolecular interactions.[21,42]

Experimentally, the rotational diffusion behavior of a chromophore is determined from TCSPC data by construction of the induced orientational anisotropy function, R(t), from the time-resolved signals for emission polarized parallel and perpendicular to the vertically polarized excitation light source,

$$R(t) = \frac{I_{\parallel}(t) - I_{\perp}(t)}{I_{\parallel}(t) + 2I_{\perp}(t)} \qquad [3.2]$$

R(t) can contain up to five exponential decays depending on the rotor shape describing solute motion and the orientation and angle between excitation and emission transition moments (δ) of the solute.[43] The information content of R(t) can, in certain cases, be sufficient to elucidate the existence of complex solvation phenomena. Despite the number of factors that contribute to the experimental R(t) signal, the most common functionality seen for the anisotropy decay is that of a single exponential.

$$R(t) = R(0)\exp(-t/\tau_{OR}) \qquad [3.3]$$

This result can be obtained either because of the rotor shape and the orientation of the transition moments of the probe molecule or due to limitations in the S/N ratio of the data. The data we report here are, to the best of our ability to determine, characterized by a single exponential decay in all cases. The functionality of the R(t) decay offers insight into the dynamics of the molecule, and the zero-time anisotropy, R(0), provides information on the spectroscopic properties of the solute. R(0) is related to the transition moment angle δ according to[44]

$$R(0) = 0.4P_2(\cos\delta) \qquad [3.4]$$

where P_2 is the second order Legendre polynomial,

$$P_2(\cos\delta) = \tfrac{1}{2}\left(3\cos^2\delta - 1\right) \qquad [3.5]$$

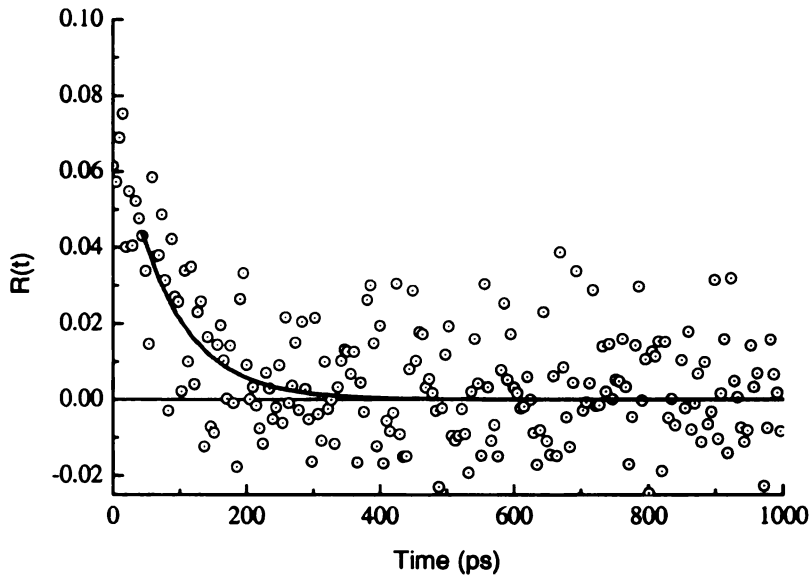

Figure 3.4 Representative experimental R(t) decay function (points) shown with regressed fit (solid line). For these data, τ_{OR} = 76 ps and R(0) = 0.08. The fitted region begins where the instrumental response function intensity is 5% of its maximum value.

Quantitating R(0) is important in reorientation measurements because variations in δ for a solute as a function of solution conditions can produce subtle changes in the form and information content of the experimental R(t) function.[45] For systems where R(0) remains essentially constant over a range of experimental conditions, the quantities τ_{OR} can be compared to one another directly. We find R(0) to be independent of solution composition for PBA, with the average angle $\delta \approx 45°$. A representative anisotropy decay curve is shown in Fig. 3.4.

The adipic acid concentration-dependence of the PBA reorientation time is presented in Fig. 3.5. The τ_{OR} data shown in Fig. 3.5 are the average of at least seven individual determinations with uncertainties reported as 95% confidence intervals. For all of the time constants measured, the experimental R(t) data were fit best by a single exponential decay. These data are consistent with PBA reorienting as a prolate rotor in aqueous adipic acid solution. We consider next the chemical information content of these data.

Equation. 3.1 predicts that an increase in the reorientation time constant can be interpreted in the context of a change in any of several quantities. Assuming constant temperature, the variable parameters are the solution bulk viscosity, η the solvent-solute friction coefficient, *f*, the solute hydrodynamic volume, V and the solute shape factor, *S*. The solution viscosity can be determined experimentally. The viscosity of aqueous adipic acid solutions at 110% of saturation (1.0 cP) is greater than that of pure water (0.89 cP) by a small amount,[46] and changes in PBA reorientation due to viscosity changes over this range would not be resolvable given our experimental uncertainty. There are two important factors contributing to the uncertainty in these data. The first is the difference in time constants for reorientation and emission processes. The fluorescence lifetime of HPBA is ~120 ns and its reorientation time in aqueous adipic acid solution is ~100 ps. This large discrepancy in time scales for the two processes produces a condition where 0.08% of the total emission intensity contains information on

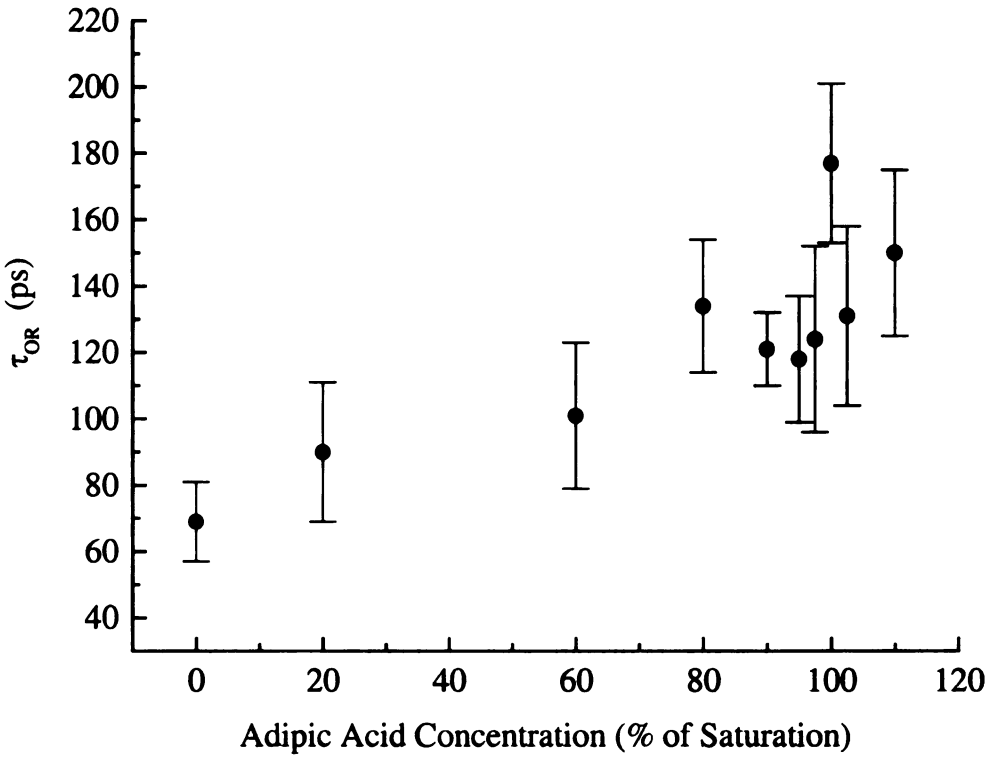

Figure 3.5 Reorientation times as a function of adipic acid concentration. The predominate species are PBA$^-$ in water (0% of saturation) and HPBA in all solutions of adipic acid. Each data point is shown with error bars at the 95% confidence limit.

molecular orientational relaxation. The second factor is the angle δ being $\approx 45°$, giving rise to an anisotropy function that is inherently small. Regardless of these factors, the adipic acid concentration-dependence of PBA reorientation cannot be rationalized in terms of a variation in solution viscosity and our previous work on PCA in adipic acid solutions has established that HPCA participates in the formation of adipic acid oligomers. Accounting for changes in PBA reorientation times as a change in *S* is

speculative considering the conformational freedom available to both solute and probe molecules. We interpret the PBA reorientation time variation with adipic acid concentration as a manifestation of oligomer formation near saturation. Oligomer formation in solution, where the probe molecule is one of the oligomer terminal units, can be modeled as a step-wise change in the hydrodynamic volume of the reorienting moiety.[27] The advantage of this approach is that it makes no assumptions about the conformation(s) of either the PBA probe molecule or the adipic acid oligomeric species.

Because we are measuring reorientation times in water, we assume that the data are interpretable in the framework of strong solvent-solute interactions, taken as the "stick" limit ($f = 1$). This solvent-solute boundary condition was shown to be appropriate for PCA reorientation in aqueous adipic acid solutions. We calculate the hydrodynamic volume of the reorienting species by adding the volume of individual adipic acid molecules (134 $Å^3$) to that of PBA (261 $Å^3$).[47] We tabulate the resulting volumes, V, and calculated reorientation times, τ_{OR}, in Table 3.1, and compare them to the experimental reorientation times. Despite the uncertainty in the conformation of the alkanoic acid side chain in PBA, we can identify two limiting cases, where the aliphatic chain is either *trans* (S= 0.623) or *cis* (S = 0.864).[29] Other, mixed conformations possess shape factors that fall between these limiting cases.

Table 3.1 Comparison of modeled τ_{OR} for PBA with addition of varying numbers of adipic acid molecules with experimentally observed values.

Adipic Acid Concentration (% Saturation)	τ_{OR} Observed (ps)	Species	τ_{OR} Calculated (ps) "cis"	"trans"
0	69±12	PBA^-	75	103
20 to110	90±21 to 150±25	HPBA + AA	113	156
		HPBA + 2AA	151	210

Comparing the experimental data to the oligomer model show close agreement at both low and high adipic acid concentrations. This agreement is based on the association of PBA with one adipic acid molecule, on average, at low adipic acid concentrations and with two adipic acid molecules at concentrations near saturation (Table 3.1). Given the uncertainty in our data and the fact that we do not have explicit knowledge of the oligomer association persistence time, we cannot provide a more detailed correlation between experiment and model. The increase in τ_{OR} with adipic acid concentration reflects association of (protonated) PBA with adipic acid and we cannot resolve whether this concentration-dependence is the result of changes in oligomer lifetime or average number, or some combination of both effects. We note that the τ_{OR} values calculated using the shape factor for the all-*cis* conformer are consistently in closer agreement with experimental values than those for the all-*trans* conformer. We believe this result to be fortuitous given the small energy difference between the conformers[48] and the inherent uncertainty in the parameters used in this model. We recognize that further information on oligomer formation might be obtained from measurements in the region between 0%

and 20% of saturation where only a 1:1 solute/probe complex may be expected to form. However, our previous work suggests that the concentrations of free PBA and the 2:1 complex would be significant and detecting a change in predominant species in this region would not be possible for reasons mentioned previously.

A major issue to be addressed in this work is the role of probe molecule structure in determining the information available from time domain experiments on solution phase organization. To that end, it is instructive to compare the results we report here on PBA to those we reported previously for PCA in the same solvent systems. Based on our data, several clear conclusions emerge; (1) It is advantageous to have the complexing moiety conjugated to the chromophore portion of the probe molecule. When this condition obtains, the steady state and transient emission responses of the probe are likely to be sensitive to complexation. (2) It is important in such experiments to obtain a reasonable match between fluorescence lifetime and reorientation time so that data acquisition can be efficient for molecular motion measurements. (3) It is important to have the chromophore portion of the probe molecule in close spatial proximity to the complexing functionality to minimize the degrees of structural freedom available to the probe and to ensure that the chromophore is sensitive to the local environment of interest.

Conclusions

We have measured the steady state and time resolved emission responses of 1-pyrenebutyric acid in aqueous adipic acid systems. The purpose of this work has been to understand the utility of this probe molecule for reporting on solute self-assembly in pre-crystallizing systems. The data we report here show the emission spectrum of PBA to be insensitive to carboxylic acid protonation and concentration of adipic acid. Fluorescence lifetime data are sensitive to both protonation of the probe carboxylic acid group and to adipic acid concentration, but the adipic acid-concentration dependence in this response can not be related clearly to the extent or nature of adipic acid organization in solution. Rotational diffusion data for PBA reveal transient association between HPBA and adipic acid, but due to the structural freedom of the probe molecule and the distance between the chromophore moiety and complexation site, the level of detail available for these measurements on local organization is limited. While this is perhaps intuitively obvious for probe molecules tethered to mesostructures characterized by moderately slow motional dynamics, to this point the correspondence of this intuition to highly dynamic molecular systems has not been made. With this information in hand, we have a better understanding of the requirements of a probe molecule for sensing solution phase self-assembly.

Literature Cited

1. Sanders, M. J.; Wirth, M. J.; *Chem. Phys. Lett.*, **1983**, *101*, 361.

2. Gudgin-Templeton, E. F.; Quitevis, E. L.; Kenney-Wallace, G. A.; *J. Phys. Chem.*,**1985**, *89*, 3238.

3. Von Jena, A.; Lessing, H. E.; *Chem. Phys.*,**1979**, *40*, 245.

4. Von Jena, A.; Lessing, H. E.; *Chem. Phys. Lett.*, **1981**, *78*, 187.

5. Eisenthal, K. B.; *Acc. Chem. Res.*, **1975**, *8*, 118.

6. Fleming, G. R.; Morris, J. M.; Robinson, G. W.; *Chem. Phys.*, **1976**, *17*, 91.

7. Millar, D. P.; Shah, R.; Zewail, A. H.; *Chem. Phys. Lett.*, **1979**, *66*, 435.

8. Blanchard, G. J.; Wirth, M. J.; *J. Phys. Chem.*, **1986**, *90*, 2521.

9. Blanchard, G. J.; Cihal, C. A.; *J. Phys. Chem.*, **1988**, *92*, 5950.

10. Blanchard, G. J.; *J. Phys. Chem.*, **1988**, *92*, 6303.

11. Blanchard, G. J.; *J. Phys. Chem.*, **1989**, *93*, 4315.

12. Blanchard, G. J.; *Anal. Chem.*, **1989**, *61*, 2394.

13. Alavi, D. S.; Hartman, R. S.; Waldeck, D. H.; *J. Phys. Chem.*, **1991**, *95*, 6770.

14. Forster, Th.; *Ann. Phys. Liepzig*, **1948**, *2*, 55.

15. Declemy, A.; Rulliere, C.; Kottis, Ph.; *Chem. Phys. Lett.*, **1987**, *133*, 448.

16. Nagarajan, V.; Brearly, A. M.; Kang, T. J.; Barbara, P. F.; *J. Chem. Phys.*, **1987**, *86*, 3183.

17. Maroncelli, M.; Fleming, G. R.; *J. Chem. Phys.*, **1987**, *86*, 6221.

18. Barbara, P. F.; Jarzeba, W.; *Adv. Photochem.*, **1990**, *15*, 1.

19. Heilweil, E. J.; Casassa, M. P.; Cavanagh, R. R.; Stephenson, J. C.; *Ann. Rev. Phys. Chem.*, **1989**, *40*, 143.

20. Hambir, S. A.; Jiang, Y.; Blanchard, G. J.; *J. Chem. Phys.*, **1993**, *98*, 6075.

21. Jiang, Y.; Blanchard, G. J.; *J. Phys. Chem.*, **1994**, *98*, 9411.

22. Jiang, Y.; Blanchard, G. J.; *J. Phys. Chem.*, **1994**, *98*, 9417.

23. Chakraborty, R.; Berglund, K. A.; *AIChE Symposium Series*, **1991**, *284*, 113.

24. Chakraborty, R.; Berglund, K. A.; *J. Crystal Growth*, **1992**, *125*, 81-96.

25. Rasimas, J.P.; Berglund, K.A.; Blanchard, G.J *J. Phys. Chem.*, **1996**, *100*, 17, 7220.

26. Rasimas, J.P.; Berglund, K.A.; Blanchard, G.J *J. Phys. Chem.*, **1996**, *100*, 17, 17034.

27. Tulock, J.J.; Blanchard G.J.; *J. Phys. Chem. B*, **1998**, *102*, 7148.

28. Flory, W. C.; Blanchard, G. J.; *Appl. Spec.*, **1998**, *52*, 82.

29. Spencer, R. D.; Weber, G.; *J. Chem. Phys.*, **1970**, *52*, 1654.

30. Mullin, J. W.; *Crystallization*, Butterworth-Heinimann, Oxford, England, 1993

31. The Merck Index, 11th Edition, Merck and Co., Inc., Rahway, NJ, 1989.

32. Debye, P.; *Polar Molecules*, Chemical Catalog Co., New York, 1929, p. 84.

33. Justus, B. L.; Cox, A. J.; Butz, K. W.; Scott, G. W.; *Chem. Phys.*, **1988**, *119*, 125.

34. Quitevis, E. L.; Horng, M.L.; *J. Phys. Chem.*, **1990**, *94*, 5684.

35. Dutt, G. B.; Doriswamy, S.; Periasamy, N.; Venkataraman, B.; *J. Chem. Phys.*, **1990**, *93*, 8498.

36. Blanchard, G. J.; *J. Phys. Chem.*, **1991**, *95*, 5293.

37. Alavi, D. S.; Waldeck, D. H.; *J. Phys. Chem.*, **1991**, *95*, 4848.

38. Vauthey, E.; *Chem. Phys. Lett.*, **1993**, *216*, 530.

39. Perrin, F.; *J. Phys. Radium*, **1934**, *5*, 497.

40. Hu, C-M.; Zwanzig, R.; *J. Chem. Phys.*, **1974**, *60*, 4354.

41. Youngren, G. K.; Acrivos, A.; *J. Chem. Phys.*, **1975**, *63*, 3846.

42. Jiang, Y.; Blanchard, G. J.; *J. Phys. Chem.*, **1995**, *99*, 7904.

43. Chuang, T. J.; Eisenthal, K. B.; *J. Chem. Phys.*, **1972**, *57*, 5094.

44. Fleming, G. R., *Chemical Applications of Ultrafast Spectroscopy*, Oxford University Press, 1986.

45. Blanchard, G. J.; Wirth, M. J.; *J. Chem. Phys.*, **1985**, *82*, 39.

46. Tulock, J. J.; Blanchard, G. J.; unpublished results.

47. Edward, J. T.; *J. Chem. Ed.*, **1970**, *47*, 261.

48. Vollhardt, K. Peter C. *Organic Chemistry*; W.H. Freeman and Company, NY, 1987; p 68.

Chapter 4

Investigating Hydrolytic Polymerization of Aqueous Zirconium Ions Using the Fluorescent Probe Pyrenecarboxylic Acid

SUMMARY

We report on the structure of primary particles produced via hydrolytic polymerization of zirconium in aqueous solutions using transient optical response of the fluorescent molecule 1-pyrenecarboxlyic acid (PCA) as a probe. We have measured the fluorescence lifetimes and rotational diffusion dynamics of PCA in aged aqueous solutions of tetravalent zirconium to understand the ability of fluorescent probes to report on the structural aspects of hydrous metal oxide self-assembly. The degree of polymerization, and therefore the level of solute organization, is controlled by allowing the Zr^{4+} solutions to polymerize, or "age", for various times at 85°C. Fluorescence lifetimes and reorientation times measured for PCA in zirconium solutions rapidly increase and approach a constant value after 30 hours of aging. The data point to growth of polymers with increased solution age and reveal that these particles achieve a constant volume. The reorientation data place limits on the size and shape of polymers and provide insight into the mechanism for their growth.

Introduction

Much research has focused on understanding the aqueous chemistry of zirconium because of its importance in a variety of applications including ceramics[1], sol-gel chemistry[2], and nuclear fuel processing[3]. In acidic solutions, it has long been accepted that zirconium exists in solution as the tetrameric species $[Zr(OH)_2 \cdot 4H_2O]_4^{8+}$ where four metal atoms are arranged nearly at right angles, joined by double bridging hydroxyl bonds[4]. Four water molecules then occupy the remaining positions of each metals coordination sphere. If solutions of zirconium are allowed to stand, these tetramer units undergo hydrolysis according to the following equilibrium:

$$[Zr(OH)_2 \cdot 4H_2O]_4^{8+} \rightleftharpoons \left[Zr(OH)_{(2+x)} \cdot (4-x)H_2O\right]_4^{(8-4x)+} + 4xH^+$$

Addition of base or heating accelerates hydrolysis, giving rise to gelatinous precipitates which, when refluxed for extended periods, produce either cubic or monoclinic hydrous zirconias[5]. Clearfield proposed a mechanism to explain these observations by assuming precipitates formed from the joining of tetrameric units through hydroxyl bridging bonds in either an ordered fashion, producing two-dimensional sheets, or randomly, resulting in three dimensional growth[5-7]. Heating of solutions was thought to allow slow growth of tetramers in an ordered fashion while addition of base was thought to cause rapid and disordered growth. Production of cubic and monoclinic phases under different experimental conditions was thought to result from ordered and random growth respectively. While there has been experimental evidence[8] to support Clearfield's theory for the formation of two-dimensional sheets, some recent data suggest that tetramers can aggregate to form rod-like particles upon heating Zr^{4+} solutions[9]. Recent literature in this area has attempted to distinguish between these several growth mechanisms.

Our interest in this chemical system stems from previous work in our laboratory that has explored the use of fluorescent probe molecules to sense solute assembly in crystallizing systems[10-13]. This strategy, termed the "Lock-and-Key" approach, relies on the use of probe molecules possessing functional groups that promote their association with the crystallizing solute. By ensuring close proximity between the probe and solute in this way, when solute organization occurs, probes experience significant changes in their local environment and exhibit changes in their steady-state and time-resolved emission responses that can be related to solute spontaneous assembly. Typically the probe is introduced as a trace impurity (~ 10^{-6} M) into solutions containing the solute. The probe chromophore emission response and rotational diffusion behavior are studied as the solute concentration is varied from below saturation through supersaturation.

We have applied this strategy to the study of self-assembly of adipic acid in aqueous solution and have found that, while fluorescence lifetimes and steady-state emission spectra report the onset of solute organization and the average environments sensed by probes, information concerning the size and structure of solute organization is derived most efficiently from rotational diffusion times. For each of these bodies of data, their information content can be optimized by careful choice of probe molecule. The level of detail that can be extracted from diffusional measurements depends, in part, on the solute identity because the exact relationship between the persistence time of transient solute organization and the time constant for reorientation of aggregates is not known. Because of this limitation, only the "average" size of adipic acid aggregates could be estimated. We have chosen aqueous solutions of zirconium as a model system for study because organization of this metal ion is known to proceed through hydrolytic polymerization

(vide infra). Once formed, solute moieties persist over long times, enabling greater correlation between probe molecule dynamics and aggregate structure. The spectroscopy of pyrenecarboxylic acid (PCA, Figure 4.1) is well characterized and was chosen as a probe for this system because of the propensity of carboxylic acids to complex[7] with Zr^{4+}

.

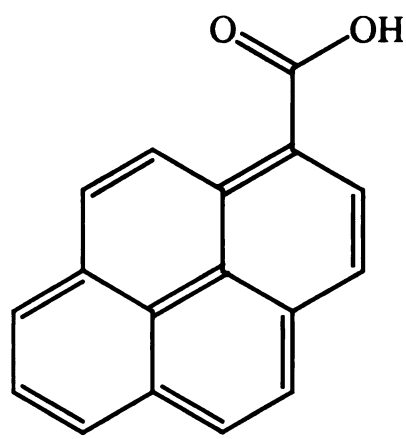

Figure 4.1 Structure of the probe molecule 1-pyrenecarboxylic acid (PCA).

The focus of the work we present here is to extend the "Lock-and-Key" strategy beyond the organic systems we have studied previously to include inorganic systems. Solutions of Zr^{4+} not only seem an appropriate choice to achieve this end (*vide supra*), but understanding the aqueous chemistry of zirconium is a matter of practical significance in the construction of robust multilayer assemblies. We have measured fluorescence lifetimes and rotational diffusion dynamics of the probe molecule PCA in solutions of Zr^{4+} aged between 0 and 110 hours to understand the limit of structural information that can be obtained from the "Lock and Key" strategy. Lifetimes were found to decrease with solution age, and the rotational diffusion behavior of PCA in these

solutions reveals that growth of zirconium hydrous polymers occurs until particles approach an upper size limit. This result is consistent with the mechanism for the precipitation of hydrous zirconias proposed by Singhal *et al.* indicating that polymers grow to form primary particles of constant size which subsequently aggregate to form crystal nuclei[9]. We find the rotational diffusion of PCA in solutions of $Zr^{4+}_{(aq)}$ senses not only the overall motion of probe/solute aggregates, but also the rotation of PCA tethered to zirconium hydrous polymers. These data, when interpreted within the model for reorientation in macromolecular and membrane systems developed by Szabo[14], place firm boundaries on the size and shape of polymers and provide evidence to indicate the most likely mechanisms for their formation.

Experimental

Chemicals: 1-pyrenecarboxylic acid (>98%) was purchased from Fluka chemical company and re-crystallized twice from methanol. The purified probe molecule exhibited a single exponential fluorescence decay in aqueous solution, as measured by single photon counting, and was judged to be pure on this basis. $ZrOCl_2 \bullet 8H_2O$ (>99.5%) was purchased from Riedel de Haën and used as received. Stock solutions of 0.2 M zirconium and 1.8 M HCl were prepared using deionized water (18 MΩ-cm; Millipore Corporation). For aging experiments, zirconium solutions were prepared by adding one equivalent of acid from to an appropriate amount of the zirconium stock solution to produce a final zirconium concentration of 0.05 M. Solutions were then "aged" at 85± 2°C using a temperature controlled silicon oil bath then removed, cooled to room temperature, and allowed stand for at least 2 hours. The probe molecule was then introduced at a concentration of 5×10^{-7} M just prior to measurement.

Time correlated single photon counting (TCSPC) spectrometer: Fluorescence lifetimes and rotational diffusion dynamics of PCA in aged zirconium solutions were measured using a time correlated single photon counting spectrometer. A detailed description of this instrument has been given in chapter 2 and only the experimental parameters important for this work are described here. A frequency doubled (532 nm), mode-locked (80 MHz), Nd:YAG laser (Quantronix 416) was used to excite a synchronously pumped, cavity-dumped dye laser (Coherent 702-2). Samples were excited by pulses of light produced by the dye laser at 646 nm (Kiton Red; R6G optics) and frequency doubled to 323nm (Type I SHG with $LiIO_3$) at a repetition rate of 8MHz. Temperature control was achieved by placing the sample cuvette in a brass block holder

maintained at 20 ± .1 °C using the output of a Neslab (model EX-221) circulating bath. Fluorescence lifetimes were recorded at a polarization of 54.7° to eliminate contributions due to rotational diffusion of the probe. Emission was collected with a subtractive double monochrometer (American Holographic B-10) at 425 nm with a 10 nm band pass.

Results and Discussion

We have obtained complementary bodies of data to characterize structure in solutions of Zr^{4+} at various stages of organization. At room temperature, organization proceeds very slowly[16] so that the extent of organization can be controlled by heating solutions for various times then cooling them to room temperature. The emission response and rotational diffusion dynamics of PCA in these "aged" solutions have been studied to evaluate the ability of fluorescent probes to report on solute self assembly. We first consider fluorescence lifetime measurements and discuss the pH-dependence of this response in terms the probe's ability to sense the completion of Zr^{4+} hydrolysis. Next, rotational diffusion data are studied to elucidate contributions to the experimental anisotropy decays from overall and internal motions of probe/solute complexes. With this information in hand, the rotational diffusion behavior of zirconium polymers is used to place boundaries on their size and shape. We consider the lifetime and reorientation data individually.

Lifetime Measurements: As mentioned previously, the polymerization of the hydrous oxide of Zr^{4+} results in a decrease in solution pH due to hydrolysis of the tetrameric species. It is important to consider that, for complex systems, fluorescent molecules can often distribute themselves in environments with properties that do not reflect the bulk composition and when this situation arises the emission properties of probes can reveal important clues about molecular scale processes. We have measured fluorescence lifetimes of PCA in buffered solutions and compared these data with those measured in aged solutions of zirconium to understand the ability of this probe to sense changes in it's local environment associated with zirconium polymerization.

As can be seen from Figure 4 2, the lifetimes of PCA in buffered solutions exhibit a measurable dependence on solution pH, varying from 5.4 ns at pH 1.7 to 5.0 ns at pH 1.1. This result cannot be explained by the simultaneous existence of two probe species in solution. If this were the case we would expect, in the limit that each form persisted much longer than their respective fluorescence lifetimes, to observe two time constants

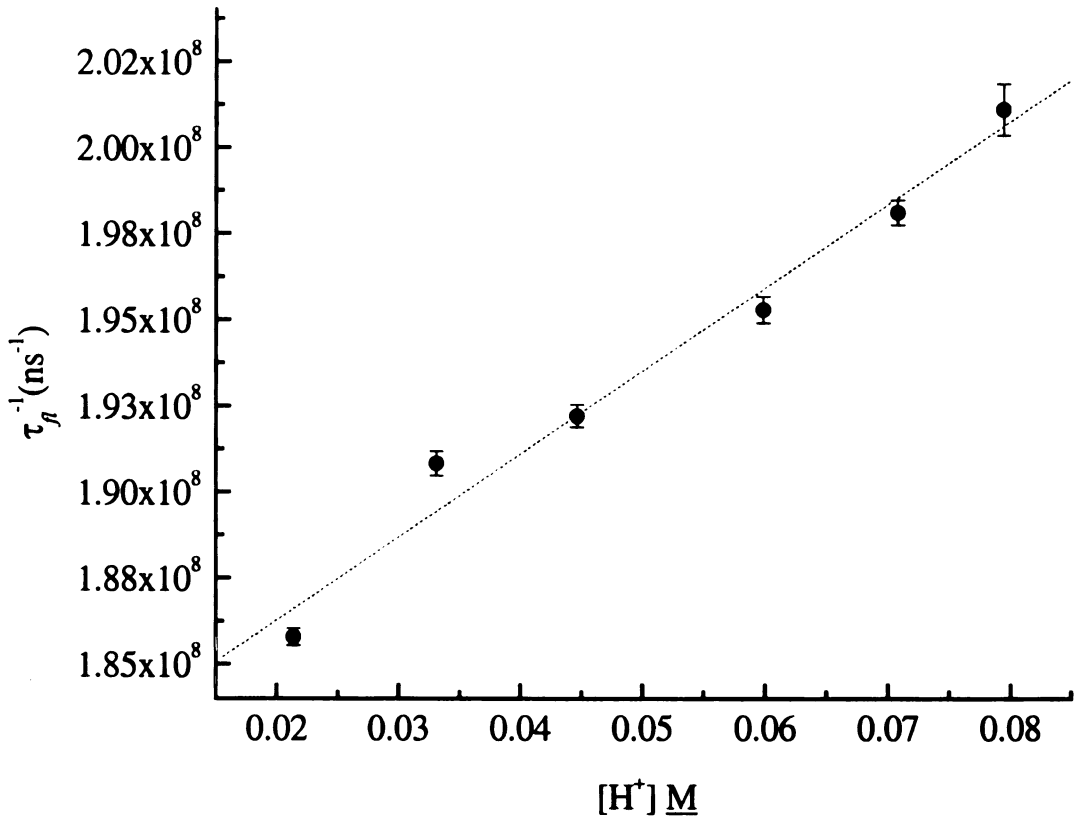

Figure 4.2 Stern-Volmer plot of fluorescence lifetime with proton concentration. Uncertainties at the 95% confidence limit are contained within each data point.

with the contribution from each being proportional to the concentration of each protonated species. Alternatively, if proton exchange were very fast compared to the fluorescence decay time constant, we would expect the observed lifetime to represent a weighted average of fluorescence lifetimes of the protonated and deprotonated forms of the probe. Although pK_a = 4. 8 for this probe, and the acid and base forms exhibit lifetimes of 5.6 and 40 ns respectively[12], it seems unlikely that this dependence is the result of a shift in equilibrium between protonated and deprotonated forms of the probe, given the fraction protonated should change by less than 0.06% over the pH range of 1.1 to 1.7. We consider that these changes result instead from quenching of PCA with increased proton concentration. For fluorophores undergoing collisional quenching, their lifetimes will depend on quencher concentration according the Stern-Volmer equation:

$$\tau^{-1} = \tau_0^{-1} + k_q[Q] \qquad [4.1]$$

where k_q is the bimolecular quenching constant, τ is the observed lifetime and τ_0 is the lifetime in the absence of quencher[17]. Figure 4.2 shows a Stern-Volmer plot of the lifetimes with increasing proton concentration. We observe a linear relationship between $\tau^{-1}$and $[H^+]$ consistent with collision quenching of PCA by protons and recover the quenching constant K_{sv} = 1.3 ± 0.2 $\underline{M}^{-1}$ and bimolecular quenching constant k_q = (2.4 ± 0.2) x 10^8 $\underline{M}^{-1}s^{-1}$. We believe quenching to be responsible for decreases in τ^{-1}that we observe in buffered solutions. With this information in hand we consider lifetimes measured in "aged" Zr^{4+} solutions.

The data in Figure 4.3 show the dependence of PCA lifetime on the age of Zr^{4+} solutions. Each data point is the result of six determinations with uncertainties reported to the 95% confidence limit.

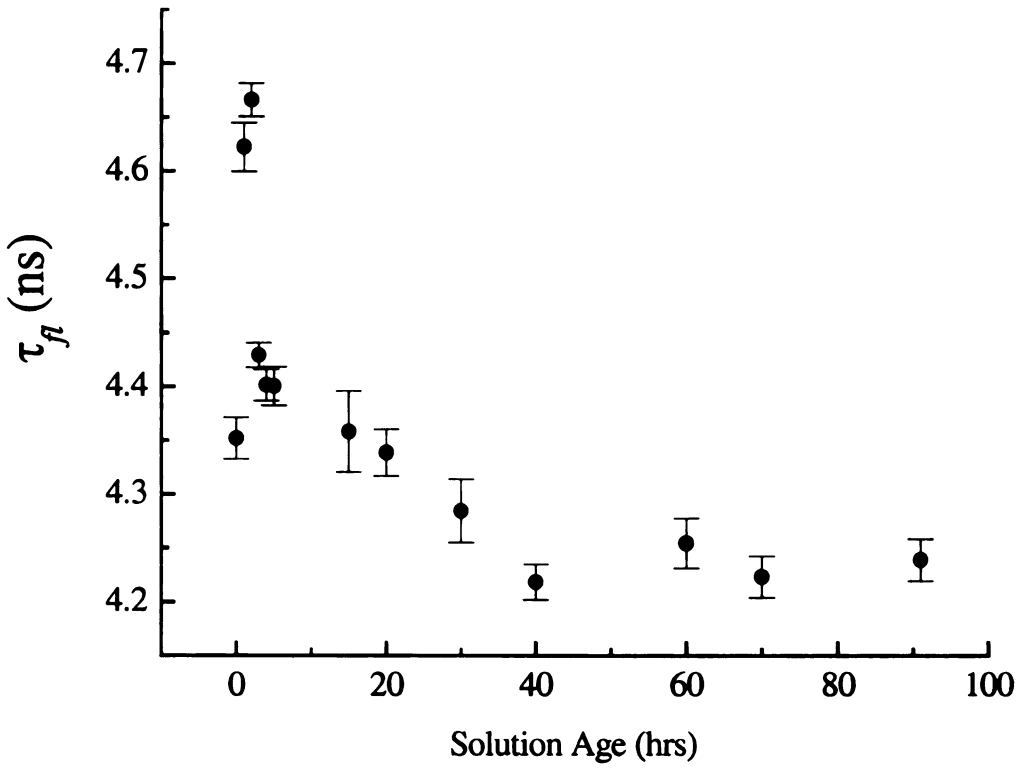

Figure 4.3 Behavior of fluorescence lifetimes with increased age of zirconium solutions. Data points are shown with error bars indicating 95% confidence intervals.

We note two important features in these data; the first is that lifetimes decrease with increasing solution age. Because pH is known to decrease with the hydrolysis of zirconium, this finding, when compared to the data for buffered solutions, indicates that the probe molecule is sensing the pH change of solution associated with the degree of polymerization. While other solution properties such as ionic strength or dielectric response may contribute to the lifetime data, it is clear that the probe molecule is

sensitive to the progress of this reaction. Examining the data further reveals that lifetimes approach a constant value, indicating polymerization to be complete to within our ability to discern after ~30 hours.

The lifetime measurements we report indicate that PCA is sensitive to the growth of zirconium polymers, most likely by sensing solution pH but, because changes in pH may result from a variety of growth mechanisms, lifetime measurements do not contain detailed information on the structure of the hydrous metal oxide polymer. In contrast, rotational diffusion measurements are sensitive to the shape of reorienting species. The geometry of polymers depends on the mechanism by which tetramer units join during polymerization and the reorientation dynamics of probes associated with these polymers should contain important structural information. The lifetime data are important, however, in providing a reference point for interpreting the reorientation data discussed below.

Rotational Diffusion Dynamics: Rotational diffusion studies have been shown to reveal important information concerning the structure of local environments experienced by probe molecules. We measure reorientation times with a time-resolved fluorescence depolarization experiment. Subsequent to polarized excitation, molecular motion causes realignment of the anisotropic chromophore ensemble. The induced orientational anisotropy function, R(t), is constructed from the experimental data according to Eq. 2.

$$R(t) = \frac{I_{\parallel}(t) - I_{\perp}(t)}{I_{\parallel}(t) + 2I_{\perp}(t)} \qquad [4.2]$$

Expressions describing the temporal behavior of R(t) have been derived by several authors[18-20]. Common to many of these treatments is the assumption that the axes for excitation, emission and diffusion bear a fixed spatial relationship in time and only

molecular motion is considered to cause depolarization of the fluorescence. For all these models, R(t) is predicted to decay as a sum of exponentials with the number of components depending on the orientations of the transition dipole moments and effective rotor shape of the reorienting moiety. The most common form of R(t) is a single exponential decay. For molecules free to reorient in solution, the orientations of the transition moments are fixed with respect to the probe geometry and single exponential anisotropy decays have typically been interpreted using the modified Debye-Stokes-Einstein (DSE) equation (Eq. 4.3) or expressions derived by Chaung and Eisenthal. Structural information is usually derived from measurements performed on solutions of varying composition and correlating accompanying changes in reorientation behavior with various solute and solvent interactions that contribute to the probe molecule local environment. The modified DSE equation relates molecular reorientation times to a number of system parameters including solution viscosity η, hydrodynamic volume of the solute V [21], Boltzman's constant k, and temperature T.

$$\tau_{OR} = \frac{1}{6D} = \frac{\eta V f}{k_B T S} \qquad [4.3]$$

Eq. 4.3 assumes ellipsoidal particles rotating in a continuum solvent. For systems where the probe is much larger than individual solvent molecules, this approximation is justified. When reorienting species approach a size comparable to individual solvent molecules, as in the case of small molecules, the solvent continuum approximation breaks down and it is necessary to introduce a phenomenological frictional term, f, to account for the effect of probe-solvent interactions. The value of f [22,23] can vary between the so-called "slip" ($0 < f < 1$) and "stick" ($f = 1$) boundary conditions and, in general, polar and non-

polar systems are best modeled in the stick and slip limits, respectively. The term S [24] is a shape factor that accounts for the non-spherical nature of reorienting moieties.

The DSE model is able to predict molecular reorientation times to within a factor of two but, because of the inherent uncertainty in parameterizing f and ambiguity in estimating V and S, the chemical information available from measurement of a single system is limited. The utility of this expression in studying complex systems rests in the prediction that reorientation times should vary predictably with bulk solution parameters such as η and T. This behavior can be used to advantage by measuring reorientation times of probe molecules in solutions of systematically varied composition. Deviations of τ_{OR} from the predictions of Eq. 4.3 can be interpreted as molecular-scale changes in any of several variables. Experiments of this nature have proven valuable in understanding the local environments experienced by probe molecules.

For simple chemical systems that exhibit reorientation dynamics characterized by more that one decay time constant, the modified DSE equation cannot be used directly. In these cases, the theory of Chuang and Eisenthal is typically used to relate the experimental data to molecular diffusional, shape and spectroscopic properties. The Chuang and Eisenthal equations have proven to be exceptionally useful in cases where solvent-dependent changes in the functionality of the probe anisotropy decay is seen [25]. These equations have been described in detail elsewhere and, in the context of this work, it is important to note that they apply for rigid systems where intermolecular degrees of freedom are restricted. For labile systems, the presence multiple components in the anisotropy decay cannot be interpreted accurately using Chuang and Eisenthal's formulation, and we need to consider this situation for the systems we report on here. We

find the reorientation of PCA in the presence of zirconium to be fundamentally different from these descriptions contained within these models, because complexation of this probe with solute molecules is such that no fixed relationship between the transition moments and diffusion axes exists. The reorientation data shown below illustrate this point.

The rotational diffusion behavior of PCA in the presence of Zr^{4+} (Figure 4.4) is very different from that in pure water (Figure 4.5). The interesting features to note from these data are the decay time constants and functionality exhibited by R(t) in each system. For pure water, R(t) decays as a single exponential with τ_{OR} ~ 90 ps (Figure 4.5b) but in freshly prepared solutions of Zr^{4+}, R(t) exhibits two decays τ_1 ~ 50 ps and τ_2 ~ 750 ps (Figure 4.4b). This change in R(t) can result only from changes in either the effective rotor shape of the reorienting moiety, the angle between the chromophore transition moments, δ, or the orientation of δ with respect to the diffusion axes. The quantity δ can be evaluated from the value of R(t) at time zero according the relationship:

$$R(0) = 0.4P_2(\cos\delta) \qquad [4.4]$$

where P_2 is the second order Legendre polynomial[26]. As can be seen from Eq. 4, R(0) depends only on δ and is independent of both the form of R(t) and rotor shape exhibited by the probe. Table 4.1 shows the behavior of R(0) to be constant for all solutions measured and we are left to consider a change in shape of the reorienting species to explain the behavior of R(t). We assert that the most likely explanation for the observed behavior of R(t) is that association of PCA with zirconium hydrous polymers produces a change the effective rotor shape of the reorienting moiety.

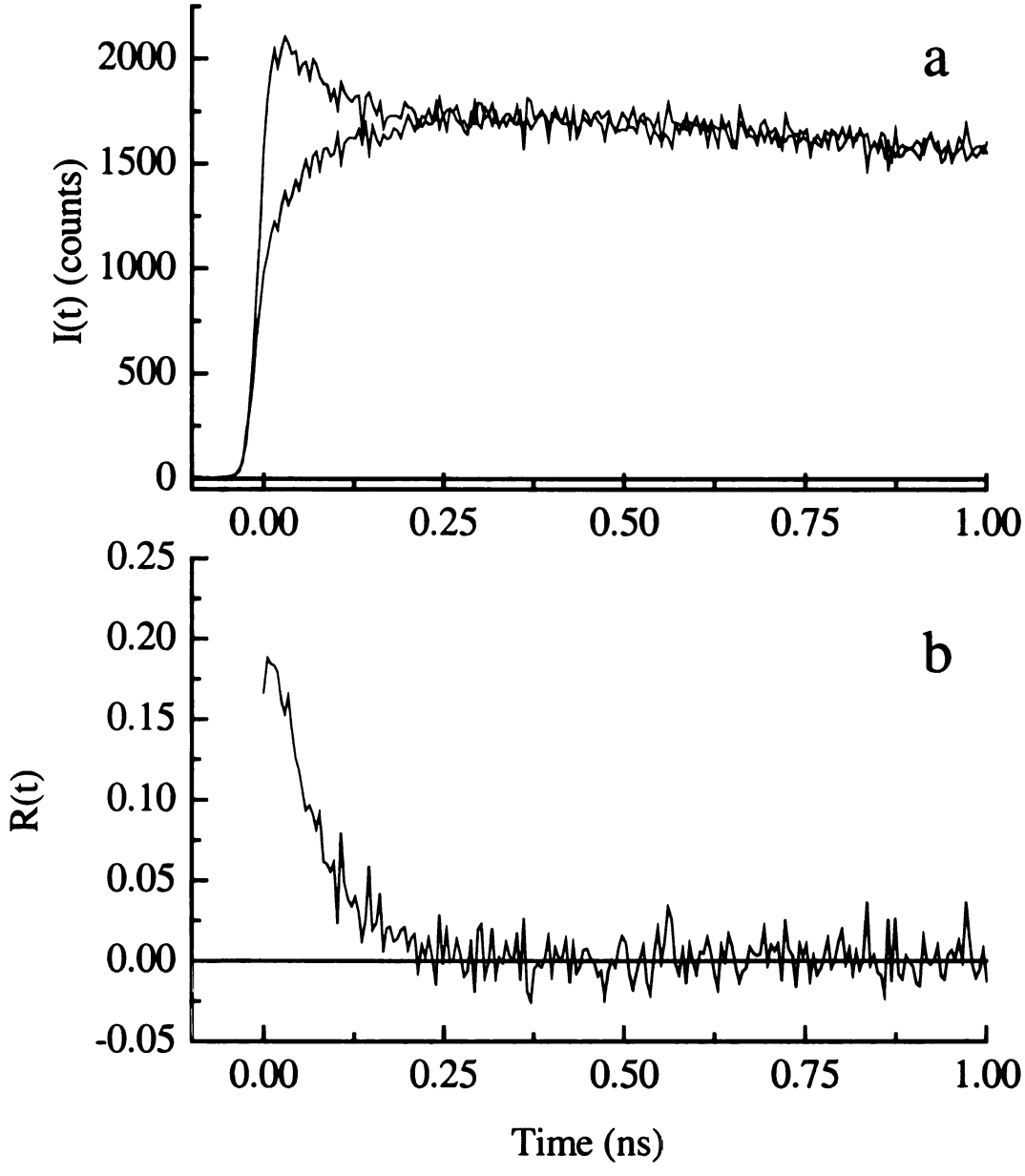

Figure 4.4 Rotational diffusion behavior of PCA in pure water (a) raw fluorescence depolarization signals $I_{\perp}(t)$ and $I_{\parallel}(t)$. (b) anisotropy function constructed from the experimental signals $I_{\perp}(t)$and $I_{\parallel}(t)$; $R(t) = 0.23\exp(-t/\tau_{OR})$.

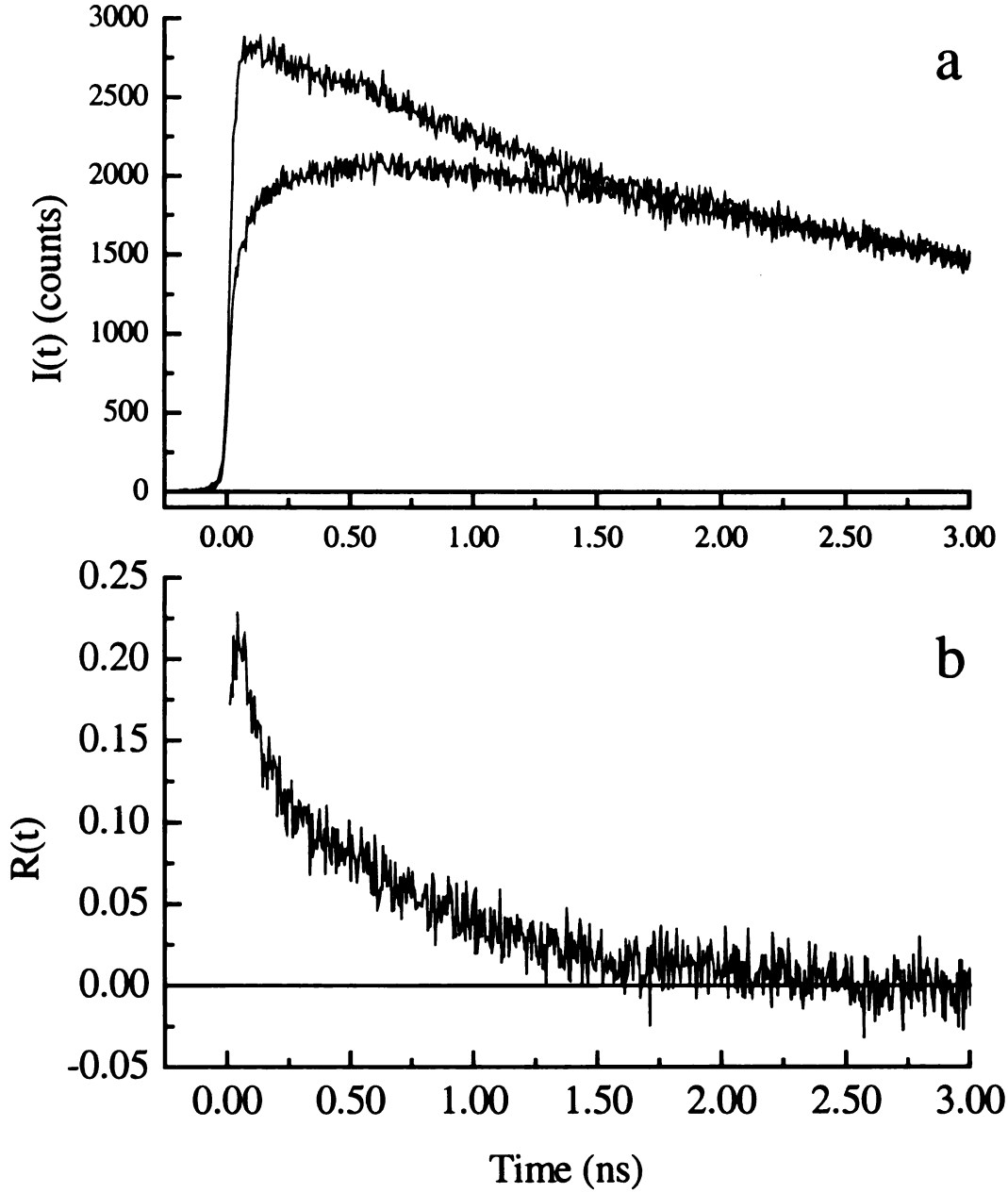

Figure 4.5 Rotational diffusion behavior of PCA in 0.05M aged zero hours (a) raw fluorescence depolarization signals $I_{\perp}(t)$ and $I_{\parallel}(t)$. (b) anisotropy function constructed from the experimental signals $I_{\perp}(t)$ and $I_{\parallel}(t)$; $R(t) = 0.17\exp(-t/\tau_1) + 0.06\exp(-t/\tau_2)$.

To this point we have not addressed the origin of τ_1 and τ_2, and making the correspondence between the time constants and the shape and size of the reorienting moiety is central to this work. While we may be tempted to attribute these decay constants to reorientation of PCA that is free in solution and complexed with the solute, $\tau_1 = 50 \pm 3$ ps (Figure 4.5) is measurably different than $\tau_{OR} = 95 \pm 18$ ps which we have measured for PCA in water (Figure 4.4). To resolve these issues, we have measured the reorientation of PCA as a function of solution "age".

The rotational diffusion behavior of PCA depends on solution "age" as shown in Figure 4.6. Each data point is the result of at least six individual measurements and the uncertainties are reported at the 95% confidence limit. A minimum of 1,000 counts were acquired in the region used for normalization of the experimental signals $I_{\parallel}(t)$ and $I_{\perp}(t)$. All decay curves were fit to both single and double exponential models and were found to fit only when two decay components were used. The quality of fit was judged on the basis that residual plots were centered about zero only for fits of double exponential decay functions.

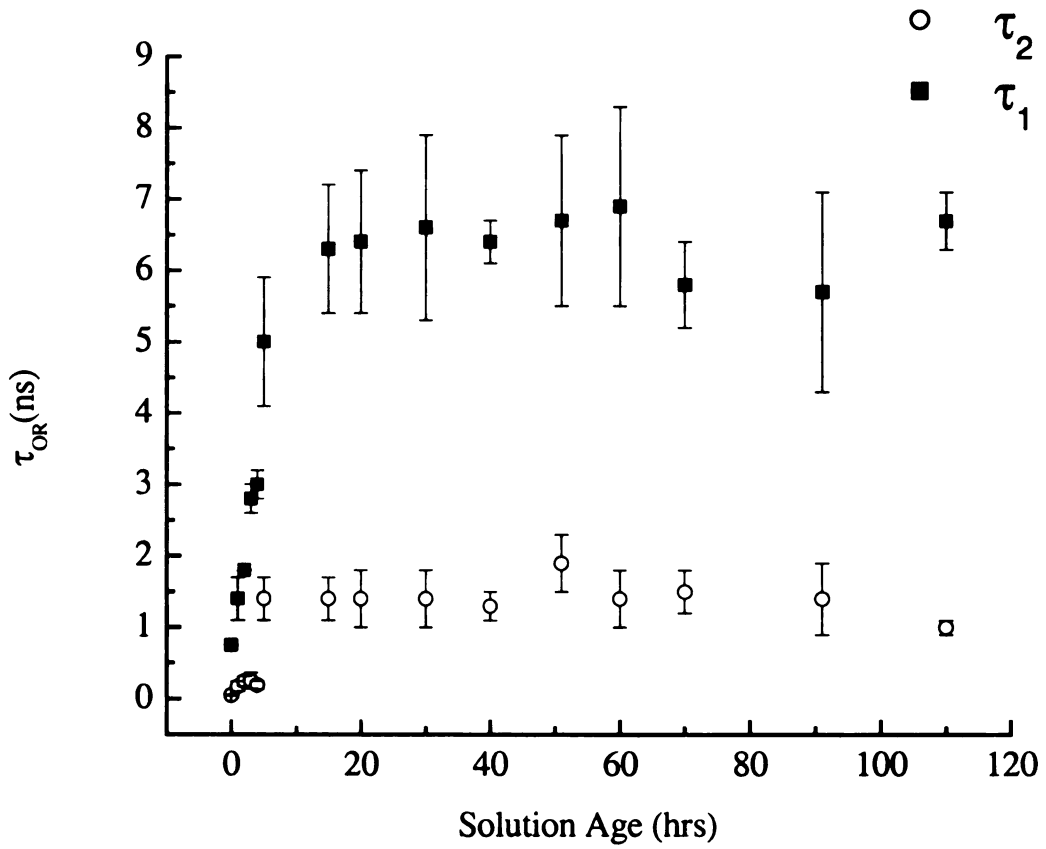

Figure 4.6 Behavior of the anisotropy decay constants τ_1 (■) and τ_2 (○) with increased age of zirconium solutions.

As can be seen from Figure 4.5, pronounced changes in τ_1 and τ_2 occur with increased solution age, with each time constant reaching a limiting value after ~ 30 hours at 85°C. The behavior of these time constants with solution "age" and their magnitude suggest that they do not originate from a mixture of free and complexed PCA. The time constants of τ_1 ~ 1.4 ns and τ_2 ~ 6.4 ns at long "age" times are not consistent with reorientation of the free probe. In order for either of these values to be consistent with

Eq. 4.3, solution viscosity would have to increase ten-fold from that of water and we observe no change in bulk viscosity with solution age. We consider the fact that both time constants increase with solution age to be consistent with the reorientation of a single moiety; PCA complexed with a oligomer, and these increases in reorientation times sense the size of solute species as polymerization proceeds. We find the reorientation times to be correlated with fluorescence lifetimes in the sense that both bodies of data indicate that growth of polymers is complete after ~30 hours of "aging".

While the reorientation data are sensitive to the growth of polymers, the relationship between τ_1 and τ_2 after 30 hours and any physical dimensions of these structures is not immediately clear. It is possible these time constants contain contributions from two types of motion: (1) overall motion of PCA/solute aggregates, (2) rotation of the fluorescent moiety relative to the zirconium hydrous polymer. In order to understand the role of these motions in determining τ_1 and τ_2 we interpret our data using the model developed by Szabo[14]. This model considers the case of reorientation of probe molecules attached to macroscopic spherical and cylindrical particles, where the probe is free to rotate about its axis of attachment to the particle. In order to relate reorientation of the transition moments to the motion of the macroscopic particles, several angles are needed to describe the relative orientations of the probe and macroscopic reference frames. Figure 4.7a shows the angles relating the orientation of the transition moments with respect to the probes reference frame. These are θ_A and θ_E, which indicate orientations of unit vectors describing the absorption (μ_A) and emission (μ_E) dipoles, respectively, relative to the probe z-axis, and ϕ_{AE}, the difference in dihedral angles between μ_A and μ_E. The probe and macroscopic reference frames are related

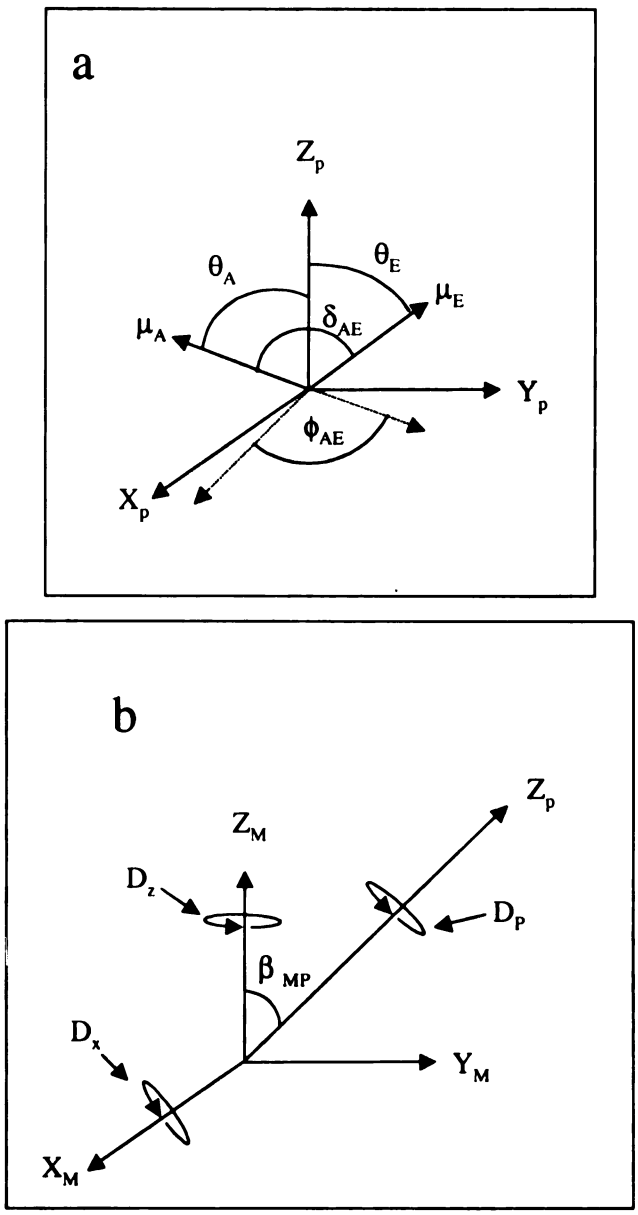

Figure 4.7 Coordinate systems showing the relationship between (a) the transition moments and a probe molecules reference frame and (b) the probe and macroscopic reference frames. The quantities θ_A and θ_E describe the orientations of the absorption (μ_A) and emission(μ_E) moments with respect the probes axis of rotation (Z_p). δ_{AE} is the angle between transition moments and ϕ is the difference between their dihedral angles with respect to the probes reference frame. β_{MP} describes the orientation of the probe and macroscopic reference frames.

through the quantity β_{MP}, which needs to be considered only for the cylindrical case, that describes the angle between the probes rotation z-axis relative to the C_∞ axis of cylindrical rotors (Z_M). Figure 4.7b illustrates the coordinate systems relating these quantities.

The Szabo model differs from Chuang and Eisenthal's treatment in that it considers the general case of fluorescence depolarization where internal motions and orientational dynamics contribute to anisotropy decays. We can reasonably assume that the probes transition moments will lie within the π-system plane of the pyrene chromophore so that ϕ_{AE} is equal to zero. Also, when Z_M is coincident with Z_P, it can be shown that for a spherical particle

$$R(t)_S = \frac{2}{5}\left[\begin{array}{l} P_2(\cos\theta_e)P_2(\cos\theta_a)\exp(-6D_M t) + \frac{3}{4}\sin 2\theta_e \sin 2\theta_a \exp(-(6D_M + D_P)t) \\ +\frac{3}{4}\sin^2\theta_e \sin^2\theta_a \exp(-(6D_M + 4D_P)t) \end{array}\right] \quad [4.5]$$

and for a cylindrical particle

$$R(t)_C = \frac{2}{5}\left[\begin{array}{l} P_2(\cos\theta_e)P_2(\cos\theta_a)\exp(-6D_z t) + \frac{3}{4}\sin 2\theta_e \sin 2\theta_a \exp(-(5D_x + D_z + D_P)t) \\ +\frac{3}{4}\sin^2\theta_e \sin^2\theta_a \exp(-(2D_x + 4D_z + 4D_P)t) \end{array}\right] \quad [4.6]$$

where D_Z and D_X are the Cartesian components of the macroscopic diffusion constant D_M and D_P is the diffusion constant for rotation of the probe molecule about Z_P (Figure 7b). It can be seen that Eqs. 4.5 and 4.6 predict R(t) can exhibit three time constants, with the first term sensing only rotation of the macroscopic particle. The second and third terms depend on both motion of the macroscopic particle and diffusion of the probe about its fixed axis. In addition, because diffusion of the probe about Z_P should be much faster than the motion of the macroscopic particle, the longest decay time constant will be

associated with the first term in all cases. It is interesting to note that, when either μ_A or μ_E are coincident with Z_P and $D_P = 0$, Eqs. 4.5 and 4.6 reduce to Chuang and Eisenthal's formulations for spherical and long axis polarized prolate rotors, respectively.

Although the above expressions predict three time constants, only two are resolved within our experimental uncertainty. This result can obtain when Z_P is closely aligned with one of the transition moments such that the amplitude of the last terms in Eqs. 5 and 6 are nearly zero. Under the condition $\theta_{A/E} \sim 6°$, we can substitute $\delta = 32°$, calculated from the data given in Table I and Eq. 4.4, into Eqs. 4.5 and 4.6, which reduces the anisotropy function in each case to:

$$R(t)_s = 0.17\exp(t/\tau_1^s) + 0.06\exp(-t/\tau_2^s)$$
$$\tau_1^s = (6D_M)^{-1}, \tau_2^s = (6D_M + D_P)^{-1} \qquad [4.7]$$

$$R(t)_c = 0.17\exp(-t/\tau_1^c) + 0.06\exp(-t/\tau_2^c)$$
$$\tau_1^c = (6D_x)^{-1}, \tau_2^c = (5D_x + D_z + D_P)^{-1} \qquad [4.8]$$

The largest contribution to R(t) is associated with the longer decay constant. This result is in agreement with the experimental values recorded in Table I, which shows two time constants at increased solution age (>30 hrs). The longer decay constant has an amplitude of ~ 0.17 while the shorter constant has an amplitude of ~ 0.06.

The importance of Eqs. 4.7 and 4.8 is that they relate the values of τ_1 and τ_2 to the macroscopic diffusion constants D_M, D_x and D_z (Figure 4.7b). By extracting values of D_M for the spherical and cylindrical cases, the DSE model can be used to estimate the volume of polymers. Clearly, these equations do not enable a distinction to be made between reorientation of probes attached to spherical or cylindrical particles. Therefore, we do not

Table 4.1 Anisotropy Data for 1-Pyrenecarboxylic Acid in Aged Solutions of Zirconium. Errors shown are at the 95% confidence limit.

Age (hrs)	τ_1 (ns)	τ_2 (ns)	R_1	R_2	R (0)
0	0.75 ± 0.01	0.047 ± 0.003	0.167 ± 0.005	0.17 ± 0.03	0.34 ± 0.03
1	1.4 ± 0.3	0.17 ± 0.07	0.18 ± 0.04	0.07 ± 0.03	0.25 ± 0.07
2	1.80 ± 0.01	0.24 ± 0.07	0.18 ± 0.01	0.052 ± 0.005	0.24 ± 0.01
3	2.8 ± 0.2	0.25 ± 0.11	0.16 ± 0.05	0.05 ± 0.02	0.22 ± 0.07
4	3.0 ± 0.2	0.19 ± 0.06	0.20 ± 0.01	0.05 ± 0.01	0.24 ± 0.02
5	5.0 ± 0.9	1.4 ± 0.3	0.16 ± 0.02	0.09 ± 0.02	0.25 ± 0.04
15	6.3 ± 0.9	1.4 ± 0.3	0.16 ± 0.02	0.09 ± 0.02	0.24 ± 0.03
20	6.4 ± 1.0	1.4 ± 0.4	0.16 ± 0.02	0.08 ± 0.01	0.24 ± 0.03
30	6.6 ± 1.3	1.4 ± 0.4	0.17 ± 0.02	0.08 ± 0.02	0.25 ± 0.04
40	6.4 ± 0.3	1.3 ± 0.2	0.16 ± 0.00	0.056±0.005	0.21 ± 0.01
51	6.7 ± 1.2	1.9 ± 0.4	0.15 ± 0.02	0.07 ± 0.02	0.22 ± 0.04
60	6.9 ± 1.4	1.4 ± 0.4	0.16 ± 0.02	0.06 ± 0.02	0.23 ± 0.04
70	5.8 ± 0.6	1.5 ± 0.3	0.17 ± 0.01	0.05 ± 0.01	0.21 ± 0.02
91	5.7 ± 1.4	1.4 ± 0.5	0.15 ± 0.05	0.08 ± 0.05	0.23 ± 0.09
110	6.7 ± 0.4	1.0 ± 0.1	0.161 ± 0.003	0.059 ± 0.006	0.22 ± 0.01

attempt to make this assignment but, by comparing the two cases, we can place limits on the size of solute organization occurring in solution. We consider these limits next.

For the spherical case, τ_1 is related directly to D_M and thus equal to τ_{OR} (Eq. 4.7). The relationship between D_M and the observed decay constants is more complicated for the cylindrical geometry, where τ_1 is equal only to the component D_x of the overall diffusion constant (Eq. 4.8). In order to calculate D_M, D_z must be known and substituted into

$$D_M = \frac{D_z + 2D_x}{3} \qquad [4.9]$$

We find that D_z is contained within τ_2 (Eq. 8) and cannot be determined independently unless D_P is known. To first order, D_P can be estimated by subtracting the reciprocal of τ_2 from that of τ_1 to give the quantity $(D_P + D_z - D_x)$. This is valid because diffusion of macroscopic particles will be much slower than rotation of the probe about Z_P.

Estimates of D_M can now be substituted into Eq. 4.3 to recover the volumes for cylindrical and spherical geometries if the shape factor of each is known. These results are summarized in Table 4.2. Calculating a volume for the spherical case is straightforward. For a spherical rotor, the time constant of 6.1 ns corresponds to a volume of 24,700 $Å^3$. For a cylindrical particle, the relationship between τ and V depends on the aspect ratio of the cylinder. For example, a rod shaped particle with an aspect ratio of 5:1 produces S = 0.22 and for 10:1, S = 0.075. These values of S yield V= 5,400 $Å^3$ and V=1,800 $Å^3$, respectively, for a reorientation time of 6.1 ns. Therefore, the volume of 24,700 $Å^3$ calculated for the spherical case must be considered the upper limit for these polymers.

Complexity arises in calculating volumes for cylindrical particles because we must consider that cylinders be described as being rod shaped or disk shaped. This would

correspond to particles having shape factors consistent with prolate and oblate ellipsoids respectively, yielding different values of *S* for a given aspect ratio. Since the dimensions of polymers should be related to those of zirconium tetramers, not all values of *S* produce volumes that are reasonable. We can place a lower limit on volume by varying S until the corresponding dimensions of each ellipsoid approach those of the tetramer (8.9Å×8.9Å×5.8Å)[8]. This treatment reveals that the volume of polymers may be as small as 4,700 $Å^3$ (prolate) or 2900 $Å^3$ (oblate).

Table 4.2 Calculated reorientation times and corresponding structural parameters for the possible polymer shapes.

	Oblate (S = 0.19)	Prolate (S = 0.11)	Sphere (S = 1)
τ_{OR}	6.1 ns	6.1 ns	6.4 ns
Volume ($Å^3$)	4,700	2,900	24,700
Tetramer Units	15	9	77
X (Å)	110	9	18
Z (Å)	9	69	18

We have stated earlier that one goal of this work is to evaluate the ability of fluorescent probes to report on the structural aspects of solute organization. With this in mind it is useful to compare the values in Table 4.2 to existing information on the size of zirconium hydrous polymers forming in solution. Clearfield has found the size of crystallites formed from zirconium solutions range in size between 48 and 96 tetramer units representing the upper limit of size polymers attain in solution[6]. The actual value must be lower than this since growth of crystallites can occur after precipitation. Our

data indicate that polymers must lie in a range between 9 and 77 tetramer units, an estimate that overlaps substantially with that made by Clearfield. We can compare our data to the result of Singhal that polymers grow initially to form rod shaped particles with a cross sectional radius of 4.3 Å[9]. This cross section corresponds to the lower bound we establish for rod shaped particles. According to the data in Table II, rod shaped particles of cross section 4.3 Å would have an aspect ratio of 5:1 and be comprised of 9 tetramer units. The above comparisons point out that the reorientation dynamics of fluorescent probes can be interpreted to provide insight into the dimensions of oligomeric species in solution.

Conclusion

We have measured the fluorescence lifetime and rotational diffusion dynamics of PCA in aged solutions of $Zr^{4+}_{(aq)}$. The lifetime data in buffered solutions reveal that this probe molecule undergoes quenching by protons at low pH. This pH-dependent response enables the probe molecule to sense hydrolysis of zirconium tetramers and the completion of their growth to form polymers. The rotational diffusion data also sense the growth of polymers and reveal that, for chemical systems where organization persists for times greater than the reorientation time of solute aggregates, detailed structural information can be obtained. Zirconium polymers were found to attain a constant size between 9 and 15 monomer units, if of cylindrical symmetry and 77 tetramer units if growth produces spherical particles. However, because spherical growth would produce polymers potentially larger that what could be supported in solution this mechanism seems least likely. We believe that solubility limits the ultimate particle size, and future efforts will center on better understanding the factors that determine the apparent size limitation for these materials.

Literature Cited

1. Dominguez-Rodriguez, A.; Gutierrez-Mora, F.; Jimenez-Melendo, M.; Routbort, J. L.; Chaim, R., *Current understanding of superplastic deformation of Y-TZP and its application to joining*, in *Mater. Sci. Eng., A*. 2001. p. 154-161.

2. Woolfrey, J. L.; Bartlett, J. R., *Processing colloidal powders, sols and gels*, in *Ceram. Trans.* 1998. p. 3-20.

3. Franklin, D. G.; Lang, P. M., *Zirconium-alloy corrosion: a review based on an International Atomic Energy Agency (IAEA) meeting*, in *ASTM Spec. Tech. Publ.* 1991. p. 3-32.

4. Mukherji, A. K., *Analytical Chemistry of Zirconium and Hafnium*. 1970, New York: Pergamon Press.

5. Clearfield, A. *J.Mater.Res* **1990**. *5*(1): p. 161-162.

6. Clearfield, A. *Inorganic Chemistry* **1964**. *3*(1): p. 146-148.

7. Clearfield, A. *Rev.Pure and Appl. Chem.* **1964**. *14*(91): p. 91-108.

8. Fryer, J. R.; Hutchison, J. L.; Paterson, R. *J. Colloid. Inter. Sci.* **1970**. *34*(238): p. 238.

9. Singhal, A.; Toth, L. M.; Beaucage, J.-s. L.; Peterson, J. *Journal of Colloid and Interface Science* **1997**. *194*: p. 470-481.

10. Rasimas, J. P.; Berglund, K. A.; Blanchard, G. J. *J. Phys. Chem.* **1996**. *100* p. 7220.

11. Rasimas, J. P.; Berglund, K. A.; Blanchard, G. J. *J. Phys. Chem.* **1996**. *100* p. 17034.

12. Tulock, J. J.; Blanchard, G. J. *J. Phys. Chem. B* **1998**. *102*: p. 7148.

13. Tulock, J. J.; Blanchard, G. J. *J. Phys. Chem. A* **2000**. *104*: p. 8340-8345.

14. Szabo, A. *Journal of Chemical Physics* **1984**. *81*(1): p. 150-167.

15. DeWitt, L.; Blanchard, G. J.; LeGoff, E.; Benz, M. E.; Liao, J. H.; Kanatzidis, M. G. *J. Am. Chem. Soc.* **1993**. *115*: p. 12158-12164.

16. Bilinsnki, H.; Durfor, C.; Tyree, S. Y. J. *J. Inorg. Nucl. Chem.* **1977**. *39*: p. 1637-1640.

17. Lakowicz, J. R., *Principles of Fluorescence Spectroscopy*. Second ed. 1999, New York: Plenum Publishers. 240.

18. Favro, D. L. *Physical Review* **1960**. *119*(1): p. 53-62.

19. Tao, T. *Biopolymers* **1969**. *8*: p. 609-632.

20. Chuang, T. J.; Eisenthal, K. B. *J. Chem. Phys.* **1972**. *57*: p. 5094.

21. Edward, J. T. *J. Chem. Ed.* **1970** *47*: p. 261.

22. Youngren, G. K.; Acrivos, A. *J. Chem. Phys.* **1975**. *63*: p. 3846.

23. Hu, C.-M.; Zwanzig, R. *J. Chem. Phys.* **1974**. *60*: p. 4354.

24. Perrin, F. *J. Phys. Radium* **1934** *5*: p. 497.

25. Blanchard, G. J.; Wirth, M. J. *J. Phys. Chem.* **1986**. *90*(11): p. 2521-2525.

26. Fleming, G. R., *Chemical Applications of Ultrafast Spectroscopy*. 1986: Oxford University Press

Chapter 5

Conclusions and Future Work

Conclusions

This thesis has demonstrated the ability of fluorescent probes to report on crystallization phenomena for a broad range of chemical systems. Aqueous adipic acid solutions were investigated using pyrenecarboxylic acid (PCA) and pyrenebutryic acid (PBA) as probe molecules, with pyrenecarboxylic acid exhibiting greater sensitivity to aggregation phenomena than pyrenebutryic acid. The fluorescence lifetimes of each of these probe molecules were found to be sensitive to concentration of adipic acid, indicating the potential for this response to report proximity to saturation. The fluorescence lifetime of PCA exhibited discontinuous behavior in the region of saturation, a result consistent with this probe being sensitive to local solute organization. The lifetimes recorded for PBA did not exhibit similar behavior.

Rotational diffusion measurements demonstrated the presence of solute aggregates at concentrations below saturation through supersaturation. The reorientation time of PCA was observed to behave in a stepwise fashion indicating the formation of solute oligomers, which increase in size with increasing adipic acid concentration. The number of solute molecules comprising aggregates was estimated from reorientation times to be approximately four, on average. The reorientation time of PBA increased in a continuous fashion with adipic acid concentration sensing the formation of solute aggregation. For each of these probes, reorientation times showed overall increases on the order of 100 picoseconds. This evidence enabled the persistence time of aggregates to be established as being $\geq$100 ps.

The differences in emission response for PCA and PBA revealed information relevant to understanding the importantance of probe structure in sensing spontaneous solute self-assembly. The steady-state and time resolved emission responses of these probes indicate that conjugation between the probe chromophore and functionalized moiety is important in determining the sensitivity of the probes emission response to aggregation phenomena. Solute organization in adipic acid solutions was found to persist over a length scale such that placing the probes chormophore at a distance of four carbon-carbon bonds limited its ability to report on solute self-assembly. This distance dependence may be different for other chemical systems and further experimentation is needed to determine this relationship unambiguously.

The hydrolytic polymerization of zirconium was investigated using PCA as a probe. The significance of this study was in demonstrating the ability of "lock and key" probes to report detailed structural information on organization in solutions. Rotational diffusion studies of this probe molecule in "aged" aqueous zirconium solutions contained rich information concerning the structure of zirconium hydrous polymers and enabled their size to be estimated. Although the shape of polymers could not be determined unambiguously, their size was established as being between 2,900 $Å^3$ and 24,000 $Å^3$ and most likely cylindrical in effective rotor shape. These results point to the potential for fluorescent probes to report the dimensions of organization for systems were aggregates persists over extended periods in solution.

Future Work

Chapter 4 of this thesis has described the investigation of the structure of hydrous oxide polymers of zirconium formed from aqueous solution. Characterizing the structure of these polymers under various conditions may play an important role in the construction of zirconium phosphate/phosphonate (ZP) multilayer assemblies. A number of chemical strategies have been employed in the construction of layered molecular assemblies[1] but ZP multilayers have gained attention because of their thermal and chemical robustness[2]. The identity of each layer in such an assembly can be controlled readily enabling their properties to be adjusted for a variety of applications[3].

One aspect of these assemblies that remains to be understood is achieving lateral control over their organization. Typically, the construction of ZP multilayer begins by phosphating the surface of a substrate such as quartz or silicon. This reaction is accomplished by treating the surface with $POCl_3$ to convert the exposed silanol groups to phosphate groups (Fig. 5.1). The resulting "primed" surface will consist of phosphate groups that are distributed statistically across the substrate surface. Multilayer assemblies are then produced by exposing the substrate alternately to solutions of $ZrOCl_2$ and organo bis-phosponates[4-6] (Fig. 5.1). As can be seen from Fig. 5.1, controlling organization vertically can be achieved but organization in the plane of the substrate cannot because of the inherently non-uniform distribution of silanol groups that are converted to phosphates[7].

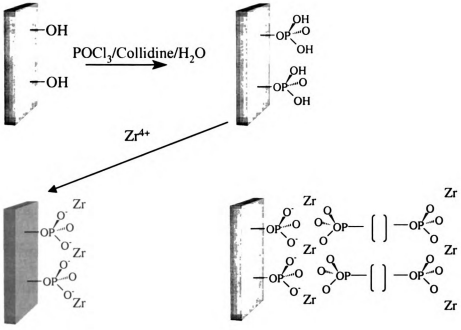

Figure 5.1 Schematic representation of ZP multilayer synthesis. The various steps shown sequentially are: phosporilation of the subtrate; zirconation of the "primed" surface; and adsorption of a generalized bis-phosponate compound. These steps are repeated to produce the desired number of layers.

Potentially, hydrous oxide polymers of zirconium could be used to template organization on phosphated or phosphonated surfaces. By allowing polymers to form in solution and subsequently depositing them on surfaces, the spatial distribution of sites available for adsorption of bisphosponates could be changed from that characterized by the silanol groups. Alternatively, zirconium could be deposited on "primed" surfaces and then polymerized by changing solution pH or heating solutions. Traditionally, zirconium has been deposited on "primed" surfaces from water/ethanol mixtures. After such an initial deposition, substrates could be removed and placed in solutions of varying ionic strength or solvent identity to promote polymerization of zirconium on substrate surfaces.

Experiments of this nature are likely to provide insight into the nature of Zr^{4+} coordination in ZP assemblies, which at present is not understood fully.

Literature Cited

1. Karpovich, D. S.; Blanchard, G. J. *Langmuir* **1994**. *10*(9): p. 3315-3322.

2. Kohli, P.; Blanchard, G. J. *Langmuir* **1999**. *15*(4): p. 1418-1422.

3. Kohli, P.; Blanchard, G. J. *Langmuir* **2000**. *16*(22): p. 8518-8524.

4. Flory, W. C.; Mehrens, S. M.; Blanchard, G. J. *Journal of the American Chemical Society* **2000**. *122*(33): p. 7976-7985.

5. Horne, J. C.; Blanchard, G. J. *Journal of the American Chemical Society* **1999**. *121*(18): p. 4427-4432.

6. Horne, J. C.; Blanchard, G. J. *Journal of the American Chemical Society* **1998**. *120*(25): p. 6336-6344.

7. Horne, J. C.; Huang, Y.; Liu, G. Y.; Blanchard, G. J. *Journal of the American Chemical Society* **1999**. *121*(18): p. 4419-4426.